LUT School of Engineering Science

Master's Degree Program in Chemical and Process Engineering

Yousuf, Alharith Asim Seidahmad

Selective Recovery of Indium From Secondary Resources by Iminodiacetic Acid Chitosan

Examiners: Associate Professor Eveliina Repo

Associate Professor Ritva Tuunila

ABSTRACT

LUT University of Technology

LUT School of Engineering Science

Master's Degree Program in Chemical and Process Engineering

Alharith Yousuf

Selective Recovery of Indium From Secondary Resources by Iminodiacetic Acid Chitosan

Master's Thesis

2019

58 Pages, 12 Figures, 9 Tables

Examiners: Associate Professor Eveliina Repo

Associate Professor Ritva Tuunila

Keywords: Indium; Adsorption; Chitosan; Iminodiacetic Acid; Isotherms; Kinetics.

Indium demand has escalated drastically in the last few decades, due to the technological advancement and the introduction of the high-tech products such as Liquid Display Panels and the mobile device; this demand is not attained due to the fact that Indium is not the sole products as it scares in the earth crust.

Indium extraction from the other mining processes side-streams, especially zinc mines is the most conventional method to produce indium, however the latter process has its drawbacks in terms of reagents loss, economical feasibility as well as the Eco-friendliness of the extraction is questioned.

This study was established to present an eco-friendly process to capture the indium ions from indium chloride solution via a biodegradable adsorbent. The primary objective of this study is to synthesize a bio-based adsorbent from biobased material (Chitosan) and eco-friendly

functionalization of Iminodiacetic Acid (IDA), thus all of the chemicals and reagents used are of a green chemistry base.

In this work IDA functionalized chitosan adsorbent was successfully synthesized, and investigated over indium chloride solution to assess the adsorption characteristics; the pH, contact time and metal concentrations. Indium uptake of IDA-chitosan was reported as 37.9 mg/g, at pH value of 3.5. The study also revealed that the indium capture by IDA-Chitosan was predicted by the Langmuir adsorption model indicating a rather homogeneous adsorbent surface, while both the diffusion and chemical reactions were effecting on the rate of the adsorption.

ACKNOWLEDGMENT

First and foremost, I want to manifest my gratitude to Dr. Eveliina Repo for introducing me to such an impressive field of the chemical process, I would also like to thank her for her precious supervision, motivation enthusiasm and her enormous cognizance of adsorption and functionalization field. Her supportive manner and her fruitful advice throughout this study, special gratitude goes to my friend Mohammad Amin Esmaielli for the supportive manner he showed towards me, also, Eveliina's research group, especially Iryna Makarava, Mohammad Reza and Vitali Kavun for their advice and help. I also am grateful to Liisa Puro and Ritva Tuunila for their brilliance cooperative work in the lab and their valuable thoughts throughout his work.

I would like to also thank my family back home, in addition to my friends and the close ones, for their support in my times of devastation and frustration, their unconditional love and their faith in my capabilities and great standby they offered.

Many thanks to my first Chemistry teacher, Mr. Abdullatif Sukit, the one who triggered the chemical engineering interest spark, the way he outstood, the way he conducts his classes and most of all the humble manner he shows whilst; I hope that am attaining some of what he has dreamt of.

I, finally dedicate this work to my late father, Asim S.Y. Surij and my Godfather, Dia S.Y. Surij, the ones who always have rendered me speechless upon their highest dose of love and faith they've had exhibited, throughout my entire life.

TABLE OF CONTENTS

Nomenclature

Symbols

β_s	Sips isotherm exponent	-
υ	Vibration	
a_L	Langmuir constant	-
B_F	Freundlich constant	-
C	Boundary layer thickness	mg/g
$C_\circ$	The initial concentration of the adsorbate	(mg/L)
C_e	The equilibrium concentration	(mg/L)
K_1	Rate constant of Pseudo-first order model	1/min
K_2	Rate constant of Pseudo-second order model	g/(mg.min)
K_F	Freundlich constant	mg/g
K_{id}	Rate constant of intra-particle diffusion	$mg/g.min^{0.5}$
K_L	Langmuir constant	L/mg
K_s	Sips affinity constant	L/mg
M	Molarity	mol/L
M	Mass	mg
q_e	Adsorption capacity at the equilibrium	mg/g
q_t	Adsorption capacity at time t	mg/g
R^2	Correlation Factor	-
t	the time interval	min
v	Volume	mL

Abbriviations

ARE	Average Relative Error
BHD	Epichlorohydrin
BPNN	Back Propagation neural network
CSIRs	Coated Solvent Impregnated Resins
CCB	Chitosan-Coated Bentonite
DTPA	Diethylenetriamine Pentaacetic Acid
EABS	The Sum of Absolute Errors
EDTA	Ethylenediaminetetraacetic Acid
EOL	End Of Life
ERRSQ	The Sum of the Square of the Errors
EGTA	Ethylene Glycol-Tetraaceticacid
FPD	Flat Panel Display
FTIR	Fourier-Transform Infrared Spectroscopy
HNT	Nano-sized Halloysite Nano-Tube

ICP	Inductively Coupled Plasma
IDA	Iminodiacetic Acid
ITO	Indium Tin Oxide
LCD	Liquid Crystal Display
LEDs	Light Emitting Diodes
MBA	Methylene Bisacrylamide
MEDCS	EDTA-cross-linked Magnetic Chitosan
MGACS	Glutaraldehyde Cross-linked Magnetic Chitosan
MPSD	Marquardt's Percent Standard Deviation
MSIRs	Modified Solvent Impregnated Resins
MWCNT	Multiwalled Carbon Nanotubes
PMA	Polymethacrylic Acid
SIR	Solvent-Impregnated Resins
TEOS	Tetraethylorthoisilicate

1 INTRODUCTION

1.1 Background

Critical metals can be defined as the valuable metals whose supply is exposed to the peril of instability and which is utilized in an important purpose based on the experts' perspective. In most of the cases, critical metals are geologically scattered on the earth, concentrated a lean geographic spots or resorted as a by-product of an other metal(Hayes and McCullough, 2018). In 2018, a draft published by federal register of U.S. comprises a list of the metals (including indium) which are deemed to be critical. Also in Finland, the EU reported a potentially discoverable indium in deposits.

As a result of the technological advancement in the flat panel displays, LCDs, Light Emitting Diodes LEDs and electro-optical devices, their market is highly expanding, as they're considered to be an environmentally friendly for their upper hand in terms of energy saving and light weight; Since indium is an essential material for the manufacturing of these devices, effective generation and recovery of this substance is in a dire need to be optimised and upgraded.

Due to the mass production of the LCDs, more attention is to be payed to the environmental issues, in this sense, recyclability is the key solution to attain the eco-friendly design. Efficient use of the available waste substance as a feed stream to generate indium will shift the indium production process into more eco-friendly regime, Furthermore, indium is both essential and rare metal that needs its consumption to be optimised the furthest it could be.

1.2 Objectives and content of research

This study is found to investigate the functionalization of Chitosan by attaching Iminodiacetic Acid to it, consecutively, testing the IDA-Chitosan adsorption properties of indium chloride solution, and to further investigate the adsorption process, including the pH dependency, adsorption isotherms, and the Kinetics study, to ultimately investigate the elusion of the indium ions from the resin.

This work comprises the literature study, and the experimental synthesis of a chitosan-IDA functionalized adsorbent and its affinity to adsorb indium from solutions; including the pH effect on the adsorption, the isotherms study and the kinetics to have a grasp on the adsorption characteristics of the synthesized sorbent and the adsorption mechanism; accompanied by desorption and regeneration study to assess the metal recovery and the reusability of the sorbent.

The theoretical aspect of this work covers a short introductory part of indium availability, production, applications in the industry, and its recovery routes, followed by a comprehended review of the previous work in indium recovery routes. Chitosan, as the base of the sorbent, also has been shortly introduced and reviewed, explaining the strong points in utilizing it as sorbent material.

In the experimental part, various methods of chitosan functionalization were studied and implemented. Fourier-transform infrared spectroscopy (FTIR) was used to verify the IDA attachment to the chitosan. Adsorption of indium from indium chloride solution was studied by the synthesized material by varying the process parameters such as pH, contact time and the initial concentration. Finally, regeneration study was conducted to test the sorbent reusability. All the experiments took place at LUT chemical engineering laboratories.

2 INDIUM

Indium – (In), is located in the third group of the periodic table of elements, its atomic weight is 114.8 while its atomic number is 49 (Busev, 1962). It was detected in a modest abundance in sulphostannates sulphogermanates, and sphalerites during a study of sphalerites by Reich and Richter in 1863, its considered one of the most rarest element as it found scattered in the earth crust and characterized by an intense blue line in the spectrum Indium is a delicate, shiny white metal with a splendid brilliance. Its plain structure gives a high pitched "cry" as the metal arched. Indium humidifies glass, as does Gallium. The earth's crust consists of 5-10 per cent by weight of indium(Fershman, 1953). It is associated most frequently with zinc materials, thus, most of the commercially produced indium is mainly obtained as a side product in zinc ores. as well as iron, lead, and copper ores.(Lide, 2005) . Indium has unique physical properties as it enhances the corrosion resistibility, strength, and the hardness of alloys with a low melting point 156.65 ℃, and an elevated boiling point 2080.05℃, whereas it becomes superconducting at -269.78 ℃ (Felix, 1990).

2.1 Availability and production

Indium (In) is not a sole product of a mining process itself, for the fact that it is not accumulated in the earth crust(Paiva, 2001). Thus, it is obtained as a by-product in the other metal productions processes i.e., zinc smelting, lead, tin and copper ores.

Generally, the primary indium production is a part of in refining process, as there are no mines with sole purpose for indium production. According to NREL report, Indium's primary production reached 770 tons, while in 2007 was only about 560 tons. This, production increase is mainly due increased demand of high-tech fields which uses indium as computer, communications and electronics and clean-energy applications like solar cells, and such demand will further increase. In terms of indium reserves, China has the largest percentage of 72% of world's confirmed reserves (Metal, 2016). With a 50-55% of global production, China Ranks first among the world producers also , followed by Belgium, Japan, Canada and south Korea. as shown in Figure 1(USGS, 2016), China production has surpassed the half of the whole world production.

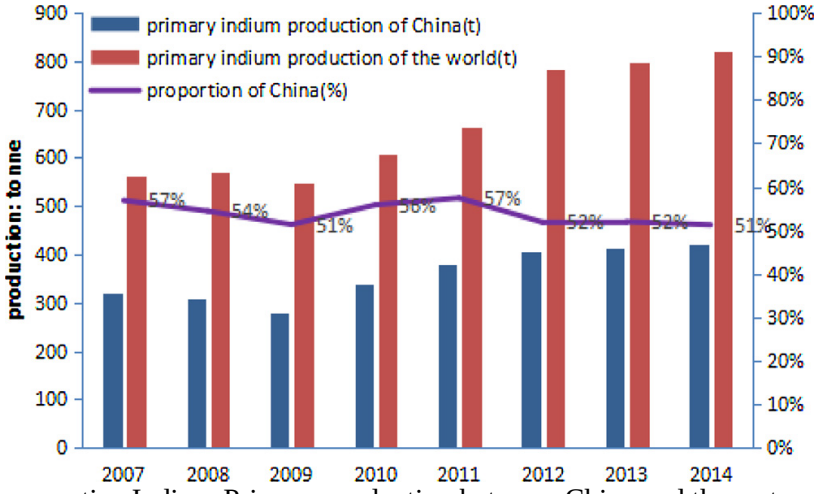

Figure 1: Comparative Indium Primary production between China and the rest world between 2007–2014(data source: USGS).

Recovery of indium from manufacturing wastes and End Of Life (EOL) products is getting much attention especially in China, Japan and south Korea. This practise is what-so called the secondary indium production which can detract from two supply sources: manufacturing process wastes such as the indium tin oxide etching processes, and old scrap, which resembles EOL consumer products, which is driven by the obsolesce and the severe damage of the aforementioned devices. (NREL, 2017).

2.2 Indium utilization aspects

The dawn of flat-panel displays played a crucial role in raising indium's commercial profile. Since the beginning of this century, a huge increment in indium production and recycling transpired. It can be remarked from Figure 2 below that the Flat Panel Displays (FPDs) industries consumes more than 50% of indium to manufacture indium tin oxide layers (ITOs), which comprises 90% indium oxide while the remaining 10% comprises tin oxide . This promotes the indium recovery from obsolete LCDs as a feasible candidate to redeem the indium supply chain in the future (Mohammad Assefi, 2018).

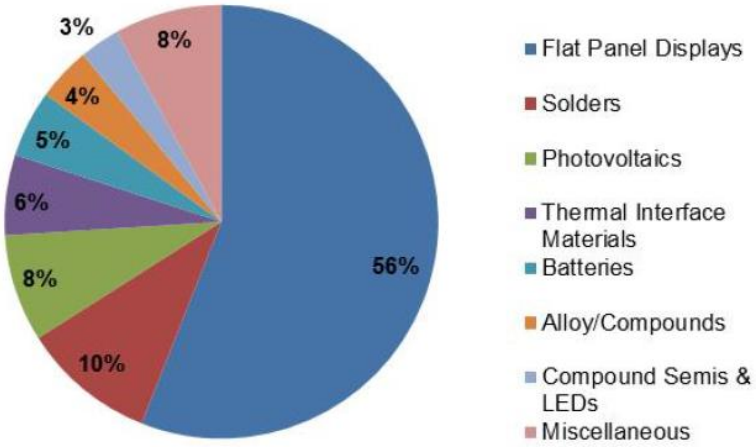

Figure 2: Indium employment(Lokanc et al., 2015)

The vast majority of indium is used in form of indium tin oxide as a translucent conductor in high-tech gadgets. With all the mentioned end uses of indium, experts have started to question the metal's future availability and supply.

2.3 Indium Supply and demand

Indium supply strongly depends on developments in zinc markets, as it is conventionally produced as a derivative of zinc mining process. Its main application is the fine electronics, hence the demand of indium is exposed to shocks in case of development of new applications. Globally, indium is roughly demanded in the range of 600-800 tons annually and anticipated to boost annually in a rate of 5% to 10% per year. Moreover, the expanded future demand exerted by the electronic industry will subject a significant pressure on the supply, as shown in Figure 3 below, although the demand surpluses the supply in the mid-first decade of the century, the metal market forecast could foresee a consequential deficit of indium supply to take place by 2020. This huge and increasing demand will induce a likely significant load on the commodity prices. Consequently, researchers got attracted by indium reclamation from the end of life indium containing devices as well as the indium etching waste streams as sources of indium recovery to redeem the indium supply(Hasegawa et al., 2013) and (Li et al., 2009).

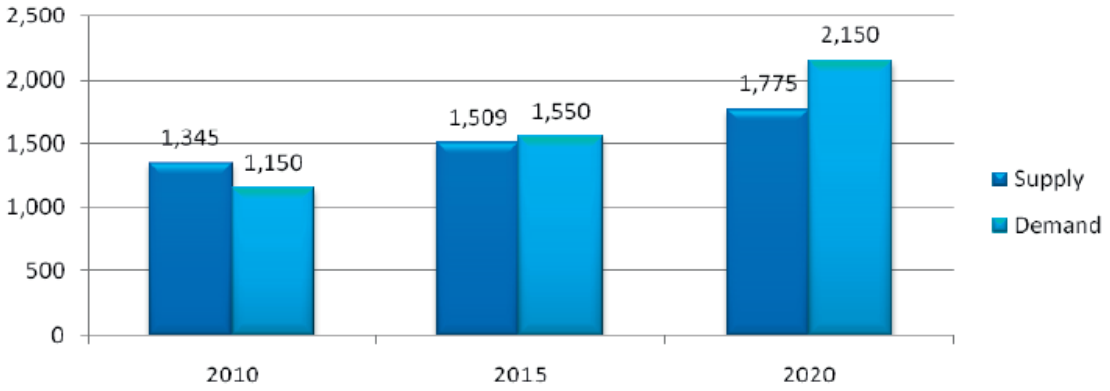

Figure 3: Indium supply and demand prognosis [Tons] (EU publications, 2011)

In 2012, Indium consumption was roughly estimated to be around 1550 tonnes, this was propelled by the manufacturing industry of liquid crystal display screens (LCD), the Flat-panel displays, touch controlled devices, computers and handled electronic devices. Over the last ten years, this electronics market has grown steadily to account for about more of the half of the total yearly consumption in ITOs form. Whereas PV demand made up almost one tenth of total consumption (Moss et al., 2012), (NREL, 2017).

3 INDIUM RECOVERY

Due to global technological progress in the technological life-style throughout the world, LCDs, cellular phone and photovoltaic cells markets nourished in an escalating manner. As per the fact that more than 50% of the indium is involved in manufacturing of the aforementioned electronic devices, especially mobile phones and LCDs, and given that the global production of this metal suffers from a clear deterioration, a deficit point will be reached in the second decade of this century. Indium recovery is the proposed to be the best way to fill this supply gap. Indium recycling can be achieved in different scales, from the recovery of mining side-steams of other metal up to the recycling of obsolete electronic devices after dismantling them and extract the indium content. In this sense, the scientists have reclaimed indium through various methods of recovery such as electrochemical methods, leaching, extraction ,and adsorption.

3.1 Indium Leaching

Indium recovery is fundamentally relying on zinc smelting process alongside the e-waste recovery. Acid leaching is the primary stage to obtain the constituents of the ITOs including indium in the liquid phase.

Many studies have investigated the indium leaching, focusing on enhancing and optimizing the process. A study by Li et al. (2006), could forthwith reclaim the indium from removed copper solution by D2EHPA at high temperatures, attaining recovery ratio of 96.25%. The abovementioned proposed process by Li et al. eliminated the iron removing step, which let to significant simplification in the process and shifted it towards the cleaner paradigm. Moreover, Li et al. (2010), investigated the indium retention from zinc oxide flue dust via oxidative pressure leaching in autoclave. The study reported that using 5.1M of the leachant for 2.5 hrs could increase the indium recovery by 13% of the atmospheric leaching. The study also deduced the oxidant optimum dosage as 0.5 and 2.5 ml/g of Hydrogen peroxide and Potassium Permanganate respectively, while the optimum leaching temperature was found to be 90 ℃. In 2011, Li et al proposed a novel procedure to leach indium from discarded indium containing devices, which consists of leaching by 100 g/L H_2SO_4 followed by precipitation with H_2S to remove the tin from the leachate, producing a sponge of indium

by zinc cementation. The study reported that indium leaching took place at 90℃ while then precipitation occurred at a partial pressure of 101.3 KPa. (Li et al., 2011).

A compact study by Yang et al. (2013), reported indium recovery by combining leaching and solvent extraction from crushed glasses using hydrochloric and sulphuric acid at 1M. The study reported full recovery of indium with purity of 99%, which was further extracted by adsorption onto chelating resins. Respectively, Yang et al. (2014), studied the consequences of the process conditions manipulation such as the pH, the concentration of the extractant, the temperature, and the contact time. The study found an efficient extraction of indium at pH <1, while the temperature increase was shown to have a positive effect on the recovery, whereas the extraction rate was found to increase by increasing of the extractant concentration (D2EHPA) by 1.5 times. Also, Li et al. (2014), concluded a compact optimization for the indium leaching using backpropagation neural network (BPNN). They reclaimed 99.5% of the indium in 2 hrs, while the optimum operation conditions were found to be the followig, residual acidity pf 50-60 g/L, 10% of oxidant content and leaching temperature of 70℃. Sawai et al. (2015), leached the indium from non ferrous smelting dust by combing several techniques, comprising chelant washing, leaching and hydroxide precipitation. After separating the coexisting lead with ethylenediaminedisuccinate (EDDS) and further leaching, 88% of the indium was recovered by hydroxide precipitation. Later, Swain et al. (2016) investigated the optimum conditions for leaching process of indium from EOL devices. The study deduced 0.07616 g/L of particle density, leaching temperature of 75℃, 400 rpm of mixing speed and 2 hrs for thorough mixing. Further hydrometallurgical methods can be used to purify the leached indium.

Combining leaching with another hydrometallurgical methods to intensify the performance has also been expansively studied. Song et al. (2020), studied indium leaching followed by two steps electrodeposition in the presence of competing positive coexisting ions such as Sn, Al and Cu. At first, the process took advantage of the high acidity and elevated temperature to precipitate the 97% of the tin ions in the leaching sequence, the indium recovery reached 99.25% at 1M of sulfuric acid and 70℃, while the electrodeposition played the major role in the extraction of Cu ions. Further studies for the electrodeposition applications to find the electric current efficiency, product purity and the rate of extraction are needed. López-Yáñez et al. (2019), studied the indium recovery using easily degradable citrates as complexing

agents (citric acid and sodium citrates). The study reported that the optimum conditions could be attained by firstly removing the competing Fe and Sn in a pre-treatment and then to leaching with 1M of citrate, 0.2M of hydrazine at pH of 5 at a solid-liquid ratio of 20 g/L. The indium recovery was reported to be more than 98% in 16.6 hrs.

3.2 Indium extraction

Indium is commonly purified by solvent extraction pathway, especially when indium is produced in zinc refineries, it is reclaimed from sulphate solution by the aforementioned process. A.M. Alfantazi (2003)focused on optimizing the extraction process to evaluate the significant parameters of it and to use them to enhance the process yield. In this regard, Liu et al. (2009) could successfully extract indium from an actual etching water of ITO process, deducing that the optimum extraction conditions were found to be 20.7 MPa and 80 ℃. The study could further capture the extracted indium utilizing $ScCO_2$ modified by fluorinated β-diketone as a chelating agent. Moreover, several chelating agents, were studied and gauged, to conclude that HFOD is the most efficient from the studied agent, achieving the maximum recovery i.e. 90.3% of indium in only 30 min. Further, Kang et al. (2011), investigated indium reclamation by solvent extraction and electrolytic refining from a doped solution that contains a variety of impurities including aluminium and molybdenum. The separation started by firstly removing the coexisting metals by dissolving the etching waste stream in sodium hydroxide, accompanied with solvent extraction of indium procuring PC88A as an extractant. The study concluded an efficient extraction of indium under acidic condition of 0.1-0.5 mol/dm^3. Pure indium was further obtained by electrolytic refining. Furthermore, Virolainen (2011), investigated the indium separation using three solvent system to reclaim the indium from tin. The study revealed an indium separation and concentration scheme from ITOs by dissolving them in 1 M of sulfuric acid, followed by D2EHPA extraction ,and selectively stripping metal by hydrochloric acid at 1.5 M. Also, Fontana et al. (2015), utilized both chemical and thermal techniques to dissolve the LCDs constituents and finally extracted the indium using PEG-based aqueous biphasic system. The study could achieve recovery above 80% of the indium at the bottom stream, while the top stream recovery was 5-20%. Whereas, Guan et al. (2015), extracted indium from wasted LCD panels and concluded indium recovery of 99% as In_2O_3 as well as comprising $InCl_3$ and InCl. The study also revealed the optimum conditions of the process as 53.91% of HCl, molar ratio of Cl/In as 11, dissolving and chlorination temperature of 400 and 500 ℃, respectively

Despite being simple and applicable method, solvent extraction is not selective, as it dissolves both the targeted material as well as the unwanted materials. Selective adsorption, in this sense can be a better candidate to redeem the indium.

3.3 Indium adsorption

Solvent extraction is a limited method in various aspects. The main shortcoming of solvent extraction process is the drainage of the reagents into solution, which leads to ecological waste production. Also, the extraction is time consuming and very complicated when a pure product is needed, not to mention the selectivity shortcoming of it. Adsorption on the contrary, is considered to be the most suitable method to recover indium for its simplicity, selectivity and eco-friendliness. Indium adsorption onto commercial resins have been focused on by many researchers, expanding the adsorption characteristics of the resins and the operating conditions (Choong Jeon, 2015).

Several papers have been published regarding indium recovery onto commercial ion exchange resins, due to the abundance of them and the easefulness of functionalization routes. Related to this, C. B. Fortes et al. (2007), investigated the indium capture on a commercial iminodiacetic acid cheating resin (Amberlite®IRC748) in a continuous mode of adsorption. The study reported final recovery rate of 99.5% of indium utilizing H_2SO_4 at flow rate of 5.0 mL/min as an eluent. Likewise, Chunhua and Caiping, investigated the indium sorption behaviour of iminodiacetic acid resin regarding different parameters. The results revealed maximum adsorption capacity of 235.5 mg/g at pH value of 4.52 and at the ambient temperature, Xiong and Yao, (2008). On the other hand, Wroński et al. (2009), modified the commercial resin of Amberlite XAD-7 with D2EHPA acid and compared it to Lewatit OC-1026 at pH value of 2.17. They reported that D2EHPA-modified resin has a greater affinity the indium than Lewatit OC-1026. Another view in to the macro-porous commercial resins,y Marinho et al. (2011) studied the indium recovery onto strong basic ion exchange commercial sorbents in the ambient conditions deducing indium uptake for them to be as follows, [.0130. 0.286, 0.270 and .320] mmol/g for Amberlite IRA–400AR, Amberlite IRA 420, Dowex 1 and Amberjet 4200 CI respectively. Further, Adhikari et al. (2012) studied the adsorption of multivalent metal ions onto calixarene-based cation exchange resins, modified by methylene crosslinking of calix(4 and 6)arene. The study reported maximum adsorption capacities of 109 and 213 mmol/g for them, respectively.

Also, Hasegawa et al. (2013) proposed a process that relies fundamentally on the quantitative capture of indium accompanied by a selective recovery of it, procuring resins comprises a wide variety of commercial resins explained in Table 1 presented at the end of this chapter, which showed a great affinity to retain the indium at rate of 97.1%. In another study, Lee and Lee, (2016) investigated Lewatit® TP207 to assess its adsorption affinity for indium. They concluded that the adsorption is governed by the pH value and the temperature, reporting indium uptake of 55 mg/g at pH value of 0.8. (Ferella et al., 2017), used a commercial resin to reclaim the metal ions from the spent electronic devices. The study investigated the adsorption of the ions onto the Amberlite (IRC748) resins, and deduced that maximum recovery of the resin was achieved at a pH value of 3, at the room temperature and in 24 hours of contact time. The captured indium could further be eluted using 2 M of sulfuric acid. Recently Assefi et al. (2018), reported the reclamation of indium using three types of macro-porous commercial resins of Lewatit and Amberlite, to conclude a proportional relationship between the adsorption efficiency and the temperature.

Indium adsorption has not been exclusive, researchers have also studied the modification of the commercial resins to enhance their adsorption characteristics as well as to improve their selectivity toward certain substances. Chang et al. (1993) achieved indium adsorption onto a synthesized chelating fibre resin and reported indium recovery ratio of 95% in the presence of competing metals such as tin, chromium and titanium. The resin could capture indium in pH range between 4-7 and in a feed flow rate of 10 mL/min. Moreover, Yuan et al. (2010), examined the coated solvent impregnated resins (CSIRs) to assess the adsorption effecting parameters. The optimal pH was observed to be 1.5. Also, Li et al. (2012)synthesized a modified solvent impregnated resins by sec-octyl phenoxy acetic acid on styrene-divinylbenzene copolymer support and tested its affinity to indium. The synthesized resin could capture indium at pH value of 3, and in a wide temperature range, with only three regeneration cycles. Respectively, Kwak et al. (2012a) studied the microbeads affinity to indium adsorption on synthesized polyvinyl phosphonic acid-co-methacrylic-acid-based. The study reported a chemisorption of the indium ions as well as adsorption capacity of 0.7 mmol/g. The same author, also achieved 0.614 mmol/g of indium onto microbeads at pH value of 3 (Kwak et al. 2012b). Additionally, Li et al. (2015), used the surface imprinting technique and indium ions as a template ion on a silica gel to synthesize indium ion imprinting polymer. Indium capture was tested in both batch and continuous process. The

study achieved indium adsorption capacity of 47.39 and 31.11 mg/g for the ion-imprinting polymer and non-ion imprinting polymer, respectively, at pH value of 3. Furthermore, Barnabas et al. (2016), investigated the indium retention in the presence of a competing ions onto a pristine Zn/Al layered double hydroxide to deduce that a high number of adsorption sites are available in the resin, resulting in a full recovery of indium and high adsorption capacity of 205 mg/g at pH value of 6. L. Timofeev et al. (2017) investigated the indium recovery using a poly-component solution that contained the ions of Iron, Zinc, and sulfuric acid as 6.2, 67. 19.6 g/dm^3, respectively, while the indium ions concentration (0.084 g/dm^3) was very small compared to these component concentrations. The study concluded that the indium sorption took place in the form of chelate complexes of di(2-ethyl-hexyl) phosphoric acid. In addition, Zichao Lia, (2019), studied -both theoretically and experimentally the adsorption behavior of indium on several chitin-based resins, to deduce a multi layer adsorption of indium onto both raw and synthesized chitin.

Some biodegradable resins have also been studied to shift the adsorption process closer to the green paradigm. A study by Calagui et al. (2014a), investigated the metal ions capture onto chitosan-coated bientonite (CCB), and reported a feasible recovery of the indium ions at adsorption capacity of 5.79 mg/g. Also, Jeon et al. (2015), performed indium adsorption using a powdered phosphorylated sawdust in batch and column process, They found that the adsorption efficiency of indium is increased as the amount of phosphorylated sawdust increase. The reported adsorption capacity was 0.95 mg/g, whereas the highest removal efficiency was 80%. Moreover, Alguacil et al. (2016), studied the adsorption characteristics of indium onto Multiwalled carbon nano-tubes (MWCNT). The investigations revealed indium recovery at adsorption capacity of 40 mg/g, moreover, the presence of other ions in the solution had a negative effect on the indium recovery. Furthermore, Akama et al. (2016), reclaimed the indium onto iminodiacetic acid-functionalized cellulose chelating cellulose. The study concluded adsorption capacity of 1.5 mmol/g at pH value of 3.5.

A compact summary of the adsorbents focused on the indium recovery is presented in Table 1. It can be observed that the commercially synthesized resins and their modified forms have outperformed the vast majority of the novel synthesized peers.

Table 1: indium adsorption by ion exchange commercial resins

Resin	Capacity[unit]	Conditions	Reference
In (III) ion & nonion-imprinted polymer	47.39 and 31.11 [mg/g] respectively	pH value of 3	(Li et al., 2015),
D2EHPA-Lewatit OC-1026	0.004 gm/cm3	Ph value of 2.17; Adsorption decrease with the increment of HCl concentration	(Wroński et al., 2009)
IDA-resin	235.5 [mg/g]	PH 4.52	(Xiong and Yao, 2008)
Ion-exchangeable nanobeads	0.78 [mmol/g]	-	(Kwak et al., 2012b)
CSIRs	26.2 [mg/g}	pH 1.5 Continuous mode. Flow rate-dependant Maximum adsorption capacity	(Yuan et al., 2010),
IRA–[400AR and 420] Dowex 1 Amberjet 4200 CI	(0.0130, 0.286, 0.270 and 0.320) [mmol/g] respectively	The whole pH range	(Marinho et al., 2011)
Chelating cellulose	1.5 [mmol/g]	pH 3.5	(Akama et al., 2016)
Metosol reagent modified with phosphoric acid and aluminium silicate	0.572–0.237 [mmol/g]		(L. Timofeev et al., 2017)
chelating fiber resin from polyacrylonitrile fiber	-	pH range of 4-7	(Chang et al., 1993)
Pristine Zn/Al layered double hydroxide	205 [mg/g]	pH 6	(Barnabas et al., 2016)
Amberlite	-	Room temperature and pH of 3	(Ferella et al., 2017)
MISRs	1.58 [mmol/g]	pH range of 3	(Li et al., 2012)
Microbeads	0.614 [mmol/g]	pH value of three temperature 293.1 K	(Kwak et al., 2012b)
Calixarene-Calix [4,6]	109 and 213 [mmol/g] respectively	pH 3	(Adhikari et al., 2012)
RMT-P	-	-	(Maeda and Egawa, 1991)
Amberlite IRC748	0.193 [mmol/g]	Dependent on the feed ratio Fe/In	(C. B. Fortes et al., 2007)

Lewatit TP [208,260] and Amberlite IRA 743	(1.488, 1.437 and 0.84) [mg/g] respectively	pH of 2 temperature of 25℃ 0.5 g resin loading.	(Assefi et al., 2018)
CCB	17.89 [mg/g]	temperature range of 278-318 K pH 4	(Calagui et al., 2014a)
Microbeads	0.7 [mmol/g]	pH 6	(Kwak et al., 2012a)
Lewatit TP207	55 [mg/g]	Acidic pH 0.8	(Lee and Lee, 2016)
Phosphorylated Sawdust	0.95 [mg/g]	25 ℃ pH of 3.5	(Jeon et al., 2015)
Carbon nanotubes	40 [mg/g]	Temperature of 60 ℃ and pH 10	(Alguacil, Lopez et al. 2016)
TE 02 MRT-SPE	0.147 [mmol/g]	-	(Hasegawa et al., 2013)
Cyanex 923 & Aliquat 336	0.45 [mol/kg]	Temperature of 303 K	(Inoue et al., 2008)
IDA-modified Chitosan	37.9 [mg/g]	pH 3.5	This study

4 CHITOSAN

Chitosan is amino based nitrogenous polysaccharide (poly-β-(1→4)-2-amino-2-deoxy-D-glucose) that is produced by the N-deacetylation of chitin (the origin compound of chitosan), which is recognized as one of the most abundant natural bio-polymers(Rinaudo, 2006). Figure 4 illustrates the structures of both chitin and chitosan. The prime origin of chitin is the aquatic life creatures, as it is found from the finest cell walls of micro-organism up to crustaceans skeleton and cartilages of shellfish. The chitin deacetylation can take place both chemically and biologically. The chemical deacetylation procures 2-5% of HCl to demineralize the feedstock, 5% NaOH for deproteinization and 40-50% of NaOH to deacetylate it into chitosan. On the other hand, the biological method of chitin acetylation utilizes organic acid-producing bacteria, protease producing bacteria, and chitin deacetylase respectively.

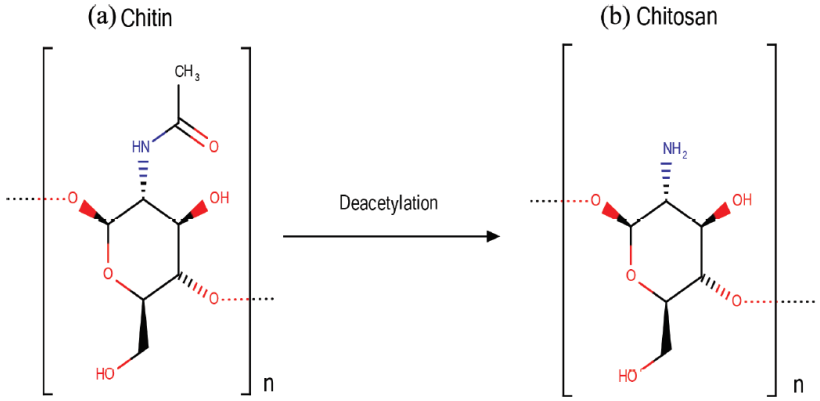

Figure 4: Structural formula of Chitin (a) and Chitosan (b) (OpenTech, 2019)

Chitosan has abundance of modifiable positions in its structural formula, what facilitated its functionalization prosperities to obtain more stable and efficient adsorbent. It is modified by either grafting or cross-linking reaction. The grafting is simply done by attaching a molecule to the chitosan functional group to multiply the number of adsorption sites. Whereas, the cross linking is done by binding the chitosan to functional groups, what terminate in a slight deterioration in the uptake capacity because of the direct bonding of the chitosan functional groups, which consequently, hinders the substance interaction (Kyzas GZ, Bikiaris, 2015).

4.1 Chitosan functionalization

Chitosan is believed to be one of the most prosperous elements in the adsorption field, due to the presence of two functionalization positions on its formula i.e. amino and hydroxyl groups, which enable the chitosan to maintain possible adsorption and functionalization interaction between the chitosan and the modification or the adsorbate. (2015). The adsorption capacity of pure chitosan to heavy metals is very deficient, thus, it can be functionalized by abundant types of both synthetic and natural polymers to improve the heavy metal uptake of it(Maity and Ray, 2018).

4.2 Chitosan based sorbents

Chitosan modification has been achieved using a wide variety of materials, for example, clay, amino-poly-carboxylic-acids (APCAs), nano composites & magnetic nano-composites, and zeolite as a functionalization groups. Below is a brief review of some relevant articles in chitosan-based sorbents(Maity and Ray, 2018).

Repo et al. (2010a) tested the modification of chitosan using Ethylenediaminetetraacetic acid (EDTA) and Diethylenetriamine Pentaacetic (Acid DTPA) and studied their affinity to cobalt and nickel. Functionalization was conducted by dissolving chitosan in acetic acid followed by dilution with methanol and EDTA or DTPA anhydride suspension in a stirred environment for several hours. After filtration, ethanol mixing and NaOH mixing the chitosan was finally dried in an oven to obtain an EDTA and DTPA functionalized chitosan. The same authors, Repo et al. (2011) took the functionalization a step further and prepared chitosan-silica hybrid material in order to make the adsorbent more rigid. The sorbent synthesis took place by a simple reaction between chitosan and tetraethylorthosilicate (TEOS) followed by the above-mentioned modification with EDTA (Repo et al., 2010a).

(Zhao et al., 2013a), functionalized chitosan by attaching ethylene glycol-bis(2-aminoethylether)-N,N,N',N'-tetraaceticacid (EGTA) chelating agents to recover Cd and Pb from their suspensions. The chitosan was modified by dissolving the chitosan and EGTA in heated water under agitation for several hours. Consequently, NaOH and (EDAC) were added respectively, agitation was maintained and the mixture was cooled down and stirred till the gelation of it. Finally, the produced material was preserved in the ambient conditions for a while followed by a soaking and washing sequence.

Another chitosan functionalization was done by Zhao et al. (2015) to study heavy metal streams recovery. Two chitosan-based sorbents were prepared: Glutaraldehyde Cross-linked Magnetic Chitosan (MGACS) and EDTA-cross-linked Magnetic Chitosan(MEDCS). MGACS was prepared by reverse-phase water to oil emulsion cross-linking mode, the chitosan was dissolved in acetic acid and the magnetic nano-particles(Fe_3O_4) were added to the solution, followed by a drop-wise water to oil emulsion, iso-hexane and emulsifiers addition to the mixture and mixed until a bright coloration of the mixture occurred. At last, the glutaraldehyde was added in a dropwise manner and the reaction was kept in refluxing mode for several hours. The MGACS was then filtered and dried in vacuum. The same procedure was followed in MEDCs modification by adding methanol-dissolved EDTA or DTPA, except that the functionalized chitosan was washed with ethanol and NaOH, deionized water, HCl and water, respectively.

Recently, (Maity and Ray, 2018), synthesized a chitosan-based nanocomposite sorbent by combining cross-linked polymethacrylic acid (PMA), nano-sized halloysite nanotube (HNT) alongside with chitosan and tested it for water treatment. The authors added oven-dried HNT and chitosan to water, respectively and mixed them at temperature of 30 ℃ until the contents dissolved. After that, methacrylic acid, and N, N'–methylene bisacrylamide (MBA) were added to the suspension. At last, potassium persulfate and sodium metabisulfite were added and the reaction was cooled, the chitosan nano-composite was filtered, washed with water-ethanol mixture for several times, and dried in a vacuum oven.

Table 2 summarizes the above mentioned functionalization routes and metal targets.

Table 2.The chitosan functionalization groups and removal of metals by the synthesized products.

Functionalization group	Adsorption Target	Capacity [unit]	Reference
EDTA and DTPA	Co (II) & Ni (II)	63.0 and 71.0 [mg/g] Accordingly	(Repo et al., 2010a)
EDTA-modified chitosan–silica hybrid materials	Heavy Metals	0.25 - 0.63 [mmol/g]	(Repo et al., 2011)
ethylene glycol-bis(2-aminoethylether)-	Cd (II) & Pb (II)	0.74 and	(Zhao et al., 2013a)

N,N,N',N'-tetraaceticacid (EGTA)		0.50 [mmol/g] Accordingly	
(MGACS) & (MEDCS)	Heavy Metals	0.878 to 1.561 [mmol/g]	(Zhao et al., 2015)
PMA/HNT	Pb (II) & Cd (II)	357.4 and 89.4 [mg/g] Accordingly	(Maity and Ray, 2018)
IDA	In(III)	37.9 [mg/g]	This study

5 ADSORPTION

Adsorption is the attachment of a certain substance from the suspension to the adsorbent surface due to the influence of a driving force (pressure or concentration). It takes place on the surface when the substance from the liquid or gas phase are attracted by the surface of the adsorbent as a result of chemical bonding or Van der Waal's attraction as per the fact that the cohesive force of the bulk is less than the former ones.

Indium is generally recovered by extraction from the by-products of zinc mining processes. This process is fragile in many technical, economical and environmental shortcomings, such as reagents losses and effluent emissions. Adsorption on the other hand, is recognized for its simplicity, selectivity, and economical and technical feasibility(Foo and Hameed, 2010b).

5.1 Adsorption fundamentals

Adsorption is categorized regarding the adsorbent-adsorbate interactions into chemisorption and physisorption. The former one takes place in correspondence of the chemical bonding amongst the adsorbent and the adsorbate in a permanent manner, hence the adsorption cannot be reversed without chemical intervention. This type of adsorption yields a significant amount of heat. Physisorption, on the other hand, occurs as a result of van der Waals interactions between the adsorbent and adsorbate, accompanied with no significant changes in the enthalpy.

The amount of the adsorbed metal at any time can be calculated from Eq. 1 below

$$q = \frac{(C_\circ - C_f) * v}{m} \quad (1)$$

$$REMOVAL\ \% = \frac{(C_\circ - C_e) * 100}{C_\circ} \quad (2)$$

Where:

$C_\circ$ is the initial concentration of the adsorbate (mg/L).

C_e is the equilibrium concentration (mg/L).

v is the solution volume (mL).

m is the adsorbent mass mg.

5.2 Adsorption isotherms

Isotherms were basically developed to study the adsorption of the gas phase substances onto activated carbon surface and then further modified to include the liquid phase adsorption as well. The fundamental definition of the isotherms study stands on the fact that for any capture of solute on solid sorbent, the residual concentration in the solution C (mol L-1), can be related to the adsorbed ions on the solid phase Q (mol kg-1). This relationship between the held up species and the remaining one is called the isotherm(Limousin et al., 2007).

5.2.1 Isotherms categorization

From the point of view that the adsorption process can take place for the three states of matter, gases, liquids and dissolved solids(Giles et al., 1974), classified the adsorption isotherms into four different subgroups, depending on the isotherm curve shape: the ‘’C’’, the ‘’L’’, the ‘’H’’, and the ‘’S’’ isotherm. Figure 5 below illustrate them.

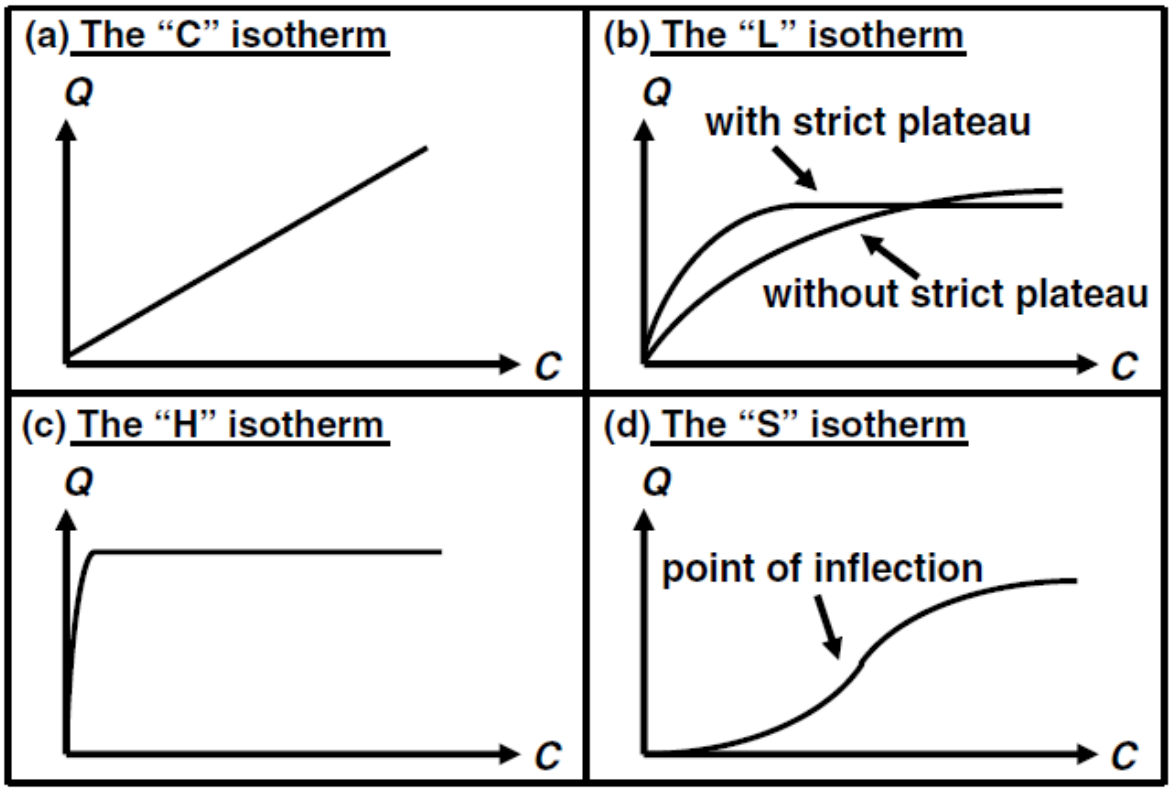

Figure 5: the primary types of isotherms (Limousin et al., 2007)

5.2.2 The ‘’C’’ isotherm

C isotherm is a simple isotherm, which is utilized in a narrow range of concentration (very dilute suspensions) as an approximation rather than an exactitude depiction. This isotherm must not be used without further verification to avoid misleading conclusions. –For example, in the case of a limited adsorption sited solid sorbent the isotherm profile can be nonlinear as a result of a probable saturation plateau. The profile, in this case, is linear intersecting the origin, which implies that the ratio of remaining species in the solution and the adsorbed ones are the equal at whichever concentration. The latter proportion is known as the partition coefficient or the distribution coefficient (Kp, Kd); Figure 5a

5.2.3 The ‘’L’’ isotherm

This isotherm assumes a gradual saturation of the solid, and it is divided based on the curve features into with and without plateau. If the curve reaches a flat horizontal trend line, the sorption capacity of the sorbent is assumed to be limited. Alternatively, the curve does not reach a levelling off point, which means the sorbent capacity is illimitable. Practically, it is very hard to tell for sure that the isotherm implies a limited or unlimited capacity. The ‘'L"

isotherm profile is a concaved line produced by the decreasing value of the ratio between the remaining species to the adsorbed when the concentration increases Figure 5b.

5.2.4 The ‘’H’’ Isotherm

The ‘’H’’ isotherm occurs when the primary slope of the ‘'L" isotherm is very precipitous. This case was recognized from the other isotherms when the solute encounters a high affinity for the sorbent and the primary gradient of the profile cannot be recognized from infinity. Hence, the H isotherm is considered as a practical case of ‘'L" isotherm

5.2.5 The ‘’S’’ isotherm

The S isotherm is a sigmoidal isotherm that transpires due to the presence of at least two counter mechanisms. A good example can be nonpolar organic compounds, which have a poor affinity with clays. However, at the moment they cover the clay surface, other organic compounds can easily be absorbed and so-called ‘'cooperative adsorption" occurs. Sigmoidal isotherm is also remarked in the presence of a soluble ligand for metallic adsorption at low concentration of adsorbate. The ligand concentration must be saturated enough to commence the adsorption typically, the inflection point in Figure 5d, depicts the point for which the adsorption conquers the complexation(Limousin et al., 2007, Allen et al., 2004).

Four types of isotherms: Langmuir, Freundlich, Redlich-Peterson and Sips were considered to study the isotherms of IDA-modified chitosan

5.3 Langmuir isotherm

Langmuir isotherm presumes a homogenous monolayer coverage of the adsorbate over the adsorbent surface (Limousin et al., 2007, Allen et al., 2004). Fundamentally, this isotherm is established on three assumptions. Firstly, it assumes the adsorption surface homogeneity so that the adsorption energy is constant throughout the whole adsorption sites. Also, the model assumes the localisation of the adsorption on the adsorbent surface, such that the adsorption takes place on a finite sites within the sorbent surface. Lastly, the model presumes the unity occupation of the adsorption sites, i.e. each adsorption site occupies by only one atom or molecule.

Graphically, Langmuir isotherm is recognized by a plateaued isotherm curve which represents the saturation point, the point above which no further adsorption will take place(Allen et al., 2004). Langmuir isotherm is represented by Eq. 3

$$q_e = \frac{K_L C_e}{1 + a_L C_e} \tag{3}$$

Where the Langmuir constants K_L& a_L, can be obtained by linearizing the fundamental equation of the model presented by Eq. 4 as follows:

$$\frac{C_e}{q_e} = \frac{1}{K_L} + \frac{a_L}{K_L} C_e \tag{4}$$

The main drawback of this model is the inefficiency in the wide concentration range as the data cannot be fitted using single set of constants.

5.4 Freundlich isotherm

Freundlich isotherm presumes incremental increase of the adsorbate deposition on the sorbent plane correspondent to the suspension concentration. Therefore the model is represented by an exponential. Hypothetically, the adoption of this model can yield in an infinite number of adsorption sites, ipso-facto, occurrence of infinite number of adsorption. This model is applied mainly in heterogeneous systems and is formulated as follows

$$q_e = K_F {C_e}^{b_F} \tag{5}$$

Where K_F and b_F are Freundlich constants that indicate the adsorption capacity and intensity respectively, and they can be driven by linearizing Eq. 5 as follows:

$$log q_e = log K_F + b_F log C_e \tag{6}$$

Freundlich equation corresponds to Langmuir model over the moderate range of concentration, nevertheless, distinctively from Langmuir equation, this model does not moderate to linear isotherm at law surface charging.

5.5 Redlich-Peterson isotherm

Redlich-Peterson isotherm is an empirical approach to represent the adsorption equilibria in a wide range of concentration. It could also be perceived as an amalgamation of Langmuir isotherm and Freundlich isotherm, as it incorporates three parameters combining elements from the both aforementioned isotherms, and it is given by Eq. 7:

$$q_e = \frac{AC_e}{1 + {C_e}^{\beta}} \tag{7}$$

The numerator is driven from Langmuir isotherm, and it approached the Henry's law at a boundless dilution limits (Nimibofa et al., 2017). The linearized form of Redlich-Peterson equation can be obtained as follows:

$$\ln(\frac{C_e}{q_e}) = \beta \ln C_e - \ln A \tag{8}$$

5.6 Sips isotherm

Sips isotherm model is a combination of Langmuir and Freundlich isotherms that is used to predict the adsorption in heterogeneous adsorption systems. It avoids the increased adsorbate concentration correlated to Freundlich. Thus, at dilute suspension it anticipates Freundlich isotherm model, on the contrary, at higher suspensions it anticipates the monolayer adsorption (Langmuir model). Sips isotherm is given by Eq. 9 .(Foo and Hameed, 2010b).

$$q_e = \frac{K_s {C_e}^{\beta s}}{1 + a_s {C_e}^{\beta s}} \tag{9}$$

Where K_s is the affinity constant, β_s is sips isotherm exponent. The model equation can be linearized as follows

$$\ln(C_e) = -\frac{1}{\beta_s}\ln\left(\frac{K_s}{q_e}\right) + \frac{1}{\beta_s}\ln(a_s) \quad (10)$$

The following table 3 summarizes the used isotherms, their model formula and the linearized formula and the plotting of the above mentioned isotherms(Foo and Hameed, 2010a).

Table 3: isotherms used in this study

Model	Fundamental formula	Linearized formula	Plot
Langmuir isotherm	$\frac{C_e}{q_e} = \frac{1}{K_L} + \frac{a_L}{K_L}C_e$	$\frac{C_e}{q_e} = \frac{1}{K_L} + \frac{a_L}{K_L}C_e$	$\frac{1}{q_e}\text{Vs}\frac{1}{C_e}$
Freundlich Isotherm	$q_e = K_F {C_e}^{b_F}$	$logq_e = logK_F + b_F logC_e$	$logq_e Vs\ logC_e$
Redlich-Peterson isotherm	$q_e = \frac{AC_e}{1 + {C_e}^{\beta}}$	$\ln(\frac{C_e}{q_e}) = \beta \ln C_e - \ln A$	$\ln(\frac{C_e}{q_e})\text{Vs}\ln(C_e)$
Sips isotherm	$q_e = \frac{q_m(K_sC_e)^{\beta s}}{1 + (K_sC_e)^{\beta s}}$	$\beta\text{s}\ln(C_e) = -\ln\left(\frac{\text{Ks}}{q_e}\right) + \ln(a_s)$	$\ln\left(\frac{\text{Ks}}{q_e}\right) Vs \ln(C_e$

5.7 Adsorption kinetics

Adsorption can be perceived as a chemical reaction between the adsorbate and the functional group of the sorbent. The adsorption kinetics is a mathematical model driven to illustrate the development of the adsorption capacity with the time to have a grasp on the adsorption reaction, hence giving a chance to access the practicable rate-controlling step (Pérez-Marín et al., 2007).

Adsorbate undergoes four consecutive theoretical adsorption steps as follows (Plazinski et al., 2009)

I. The solute transportation within the bulk of the solution.
II. The solute transportation crosswise the liquid film embracing the sorbent.
III. The solute diffusion in pore structure of the sorbent, i.e. (intra-particle diffusion).
IV. Solute adsorption on the surface of the sorbent.

5.7.1 Pseudo first-order model

Also know by Lagergren model (Sen Gupta and Bhattacharyya, 2011), proposed by Lagergren at the end of the 19th century as an empirical equation for the rate of the oxalic and malonic acid adsorption onto charcoal, it is one of the earliest equation to illustrate the liquid-phase systems (Plazinski et al., 2009). The derivation of the formula is shown as follows:

$$\frac{dq}{dt} = k_1 (q_e - q) \tag{11}$$

$$(q_e - q)\, dq = k_1\, dt \tag{12}$$

By integrating Eq. 12

$$\int_0^{q_t} \frac{1}{(q_e - q)}\, dq = \int_0^t k_1\, dt \tag{13}$$

$$ln(q_e - q_t) = \ln(q_e) - k_1 t \tag{14}$$

$$\log (q_e - q_t) = \log(q_e) - \frac{k_1}{2.303}\, t \tag{15}$$

Where

q_e is the adsorbed substance at the equilibrium [mg/g]

q_t is the amount of the adsorbed substance at time t [mg/g]

t is the time interval [min]

And the parameters k_1 and q_e are determined by using linear regression

5.7.2 Pseudo second-order model

This model is used to demonstrate adsorption which includes chemisorption as in the case of second order, yet in a different idea of it (Ho, 2006). It presumes that the rate determining step is dependent on the surface reaction (Zhao et al., 2013a). The pseudo second order equation is derived as follows:

$$\frac{dq}{dt} = k_2\,(q_e - q_t)^2 \tag{16}$$

$$\int_0^{q_t} (q_e - q_t)^{-2}\, dq = \int_0^t k_2\, dt \tag{17}$$

$$-\frac{1}{q_e - q_t} + \frac{1}{q_e} = k_2 t \tag{18}$$

$$-1 + \frac{q_e - q_t}{q_e} = k_2 t q_e - k_2 t q_t \tag{19}$$

$$q_t = k_2 t {q_e}^2 - k_2 t q_t q_e \tag{20}$$

$$\frac{q_t}{q_t k_2 {q_e}^2} = \frac{k_2 t {q_e}^2}{q_t k_2 {q_e}^2} - \frac{k_2 t q_t q_e}{q_t k_2 {q_e}^2} \tag{21}$$

$$\frac{t}{q_t} = \frac{1}{k_2 {q_e}^2} + \frac{1}{q_e} t \qquad (22)$$

The kinetics study can help to understand and determine the adsorption mechanisms depending on the best representation of the experimental readings, i.e., pseudo first order implies that the process mechanism follows mono-site occupancy of the adsorbate, whereas, pseudo-second order predicts two site occupancy.

5.7.3. Intraparticle diffusion model

Introduced to describe the pure diffusion at first, afterwards it was expanded to describe the diffusion-controlled liquid/solid adsorption models. The model is presented by the following formula.

$$q_t = k_{id} t^{1/2} + C \qquad (23)$$

Where

k_{id} is the constant of intra-particle diffusion (mg/g min0.5).

C is the boundary layer thickness (mg/g).

5.8 Error analysis

Recently, linear regression has gained the attention as one of the most viable tools applied in the experimental data (adsorption data) analysis, as it has been utilized in the definition of the best relationships for data fittings to quantify the adsorbates distribution as well as the adsorption models consistency verification (Nimibofa et al., 2017). This linearization of the adsorption isotherms data implies data transformation. Therefore it will induce alteration in the error structure and may lead to violation in the error variance, as well as the normal assumption of the standard error function i.e., least square values (Allen et al., 2004).

In contrast to linear regression, nonlinear regression, based on its convergence criteria, minimizes the error dissemination amidst the isotherm and the experimental readings (Nimibofa et al., 2017).

5.8.1 The sum of the square of the errors (ERRSQ):

The sum of the square of the errors is considered the most commonly used formula in adsorption parameters derivation, and it is given by Eq. 11.

$$ERRSQ = \sum_{i=1}^{n} (q_{e\,exp} - q_{e\,model})^2 \quad (24)$$

Where $q_{e\,exp}$ & $q_{e\,model}$ are the experimental and modelled adsorption capacities respectively and n is the number of the readings.

The above mentioned error function is believed to be the most common one to use, however, the parameters are calculated by the magnitude of the errors, hence, ERRSQ will bias the fit favouring the higher concentrations data (Ng et al., 2002).

5.8.2 The Hybrid Fractional Error Function (HYBRID)

Hybrid fractional error function was introduced as a trial to enhance the sum of squares error formula fit at low concentrations., The modification introduced was by dividing the latter one by a measured value, more to add, this function comprises the number of degrees of freedom of the system i.e., the subtract of the number of the data and the number of the parameters of the isotherm model. The formula of the function is presented as follows:

$$HYBRID = \frac{100}{n-p} \sum_{i=1}^{n} \left[\frac{(q_{e\,exp} - q_{e\,model})}{q_{e\,exp}} \right] \quad (25)$$

Where p is the number of the model's parameters and n is the number of readings.

5.8.3 The sum of absolute errors (EABS).

EABS is similar to the sum square error function (ERRSQ), yet, it is used to give a better fit than EESQ, because the errors magnitude increases favouring the fit to approach the high concentrations readings.

$$EABS = \sum_{i=1}^{n} \left| q_{e\,exp} - q_{e\,model} \right| \tag{26}$$

5.8.4 Average Relative Error (ARE)

In this error function, the fractional error distribution is minimised throughout the whole concentration range, the formula of function is given as follows:

$$ARE = \frac{100}{n} \sum_{i=1}^{n} \left(\frac{\left| q_{e\,exp} - q_{e\,model} \right|}{q_{e\,exp}} \right) \tag{27}$$

5.8.5 Marquardt's Percent Standard Deviation (MPSD)

Is analogous to a geometric mean error distribution modified in accordance to the degree of freedom of the system, and is represented by:

$$MPSD = \frac{1}{n-p} \sum_{i=1}^{n} \sqrt{\left(\frac{\left(q_{e\,exp} - q_{e\,model} \right)}{q_{e\,exp}} \right)^2} \tag{28}$$

Selection of the error function is a crucial step in the parameter derivation as it can affect the obtained parameters, which can be misleading if the error functions are misused. Table 4 depicts five different error functions that are usually utilized to obtain the isotherms model's parameters.

Table 4:the error functions used in this study

Error function name	Abbreviation	Formula
The sum of the square of the errors	(ERRSQ)	$\sum_{i=1}^{n} (q_{e\,exp} - q_{e\,model})^2$
The Hybrid Fractional Error Function	(HYBRID)	$\frac{100}{n-p} \sum_{i=1}^{n} \left[\frac{(q_{e\,exp} - q_{e\,model})}{q_{e\,exp}} \right]$

Sum of Absolute Errors	(EABS).	$\sum_{i=1}^{n} \left\| q_{e\ exp} - q_{e\ model} \right\|$
Average Relative Error	(ARE)	$\frac{100}{n} \sum_{i=1}^{n} \left(\frac{\left\| q_{e\ exp} - q_{e\ model} \right\|}{q_{e\ exp}} \right)$
Marquardt's Percent Standard Deviation (MPSD)	(MPSD)	$\frac{1}{n-p} \sum_{i=1}^{n} \sqrt{\left(\frac{\left(q_{e\ exp} - q_{e\ model} \right)}{q_{e\ exp}} \right)^2}$

6 EXPERIMENTAL PART

The experimental work consisted of the modification of chitosan using iminodiacetic acid as a functional group. The characterization of the functional group attached to the sorbent surface was verified using FTIR. All the weighing procedures (chemicals and sorbent dosage) were done using a standard scale of (METTLER AE240), while liquid measurements were done with the glass pipettes. The pH values were recorded by Metrohm 744 pH meter and the temperature was adjusted by a mercury thermometer scale. As for the adsorption, the process took place at ambient conditions and in batch mode using 10 mL tubes. The mixing was carried out by a shaker mixer EDMUND BULER KS10 at a constant rotation of 350 rpm in all of the experiments. After preparing and procuring the sorbent in an adsorption process, the final test to complete the recovery cycle of the metal was to elude the captured ions. Desorption study was undertaken to determine the elution characteristics and the reusability of the resins accordingly.

After the adsorption processes, the sorbent was separated using a syringe filter with a pore size of 0.45µm. Consequently, both the filtered and the prepared sample were analysed by inductively coupled plasma ICP (AGILENT TECHNOLOGIES 7900) to determine the metal ions concentrations before and after the adsorptions, the ICP unit calibrate the tested samples to a previously fed data of a calibration curve prepared by a matrix solution obtained by mixing 1% volume of each of (hydrochloric and nitric) acid in deionized water. The data obtained from the ICP tests were collected and treated and used to describe the adsorption process of indium ions onto IDA-functionalized chitosan using the previously mentioned equations.

6.1 Materials and methods

6.1.1 Chemicals and reagents

Sigma Aldrich provided each of Chitosan powder ((Poly(D-glucosamine) Deacetylated chitin), 90-100 % w of epichlorohydrin (1-Chloro-2,3-epoxypropane) and indium chloride powder (InCl3). While 98% w of Iminodiacetic acid (IDA) and 98-100% of Sodium hydroxide pellets were procured by Fisher Scientific and VWR respectively. All the

chemicals procured in this study were of a reagent grade and used without further purification.

6.1.2 Chitosan functionalization

The functionalization method was adopted from Razak et al. (2018) with some manipulation of the quantities of the chemicals, by dissolving 10 grams of iminodiacetic acid and 10 mL of Epichlorohydrin (BHD) in 50 mL of water that contained 5 grams of dissolved sodium hydroxide. The mixture was stirred for 4 hours at 400 rpm, using a magnetic stirrer in an oil bath, and at 60℃. 4 more grams of NaOH was added to the stirred system till they were completely dissolved and then 5 grams of chitosan powder were added with elevating the temperature to 85 ℃ and decreasing the agitation speed to 300 rpm to avoid the breaking of the chitosan due to the hostile environment. The chitosan was then filtered in a Buchner filter and washed several times with 0.5M HCl accompanied with demineralizer water washing sequence twice. The chitosan was filtered and dried in an oven at 90 ℃ for 24 h. The IDA-functionalized Chitosan was a dark yellowish powder.

6.1.3 Indium solution preparation

The indium solution was obtained by dissolving indium chloride powder in distilled water with respect to the indium valence in the chemical formula, the initial concentration of the indium solution was 400 mg/L, and then diluted to obtain the needed concentrations for the isotherm and kinetics studies

6.1.4 Indium solution pH adjustment

The pH is believed to be one of the most compelling element on the sorption behaviour by the nature of the protonation and deprotonation of the functional groups of IDA-chitosan resin. pH was studied by over pH range of 0-4 while keeping the other factors constant. (Resin loading 10 mg, concentration 30 mg/L and time 24 hr).

The pH adjustment of the working solution encountered a speciation in the indium solution and assumed to be indium hydroxide, this assumption was confirmed by referring to the available literature, as reported by Assefi et al. (2018), who concluded, based on an obtained Eh-pH diagram that there is a different speciation of indium ions ($InCl_3$, $In(OH)_3$ and In_s)

phases in a wide range of pH. The following diagram in Figure 6 shows that the indium solution tends to speciate from In(III) to $In(OH)_3$ in pH range above 4.

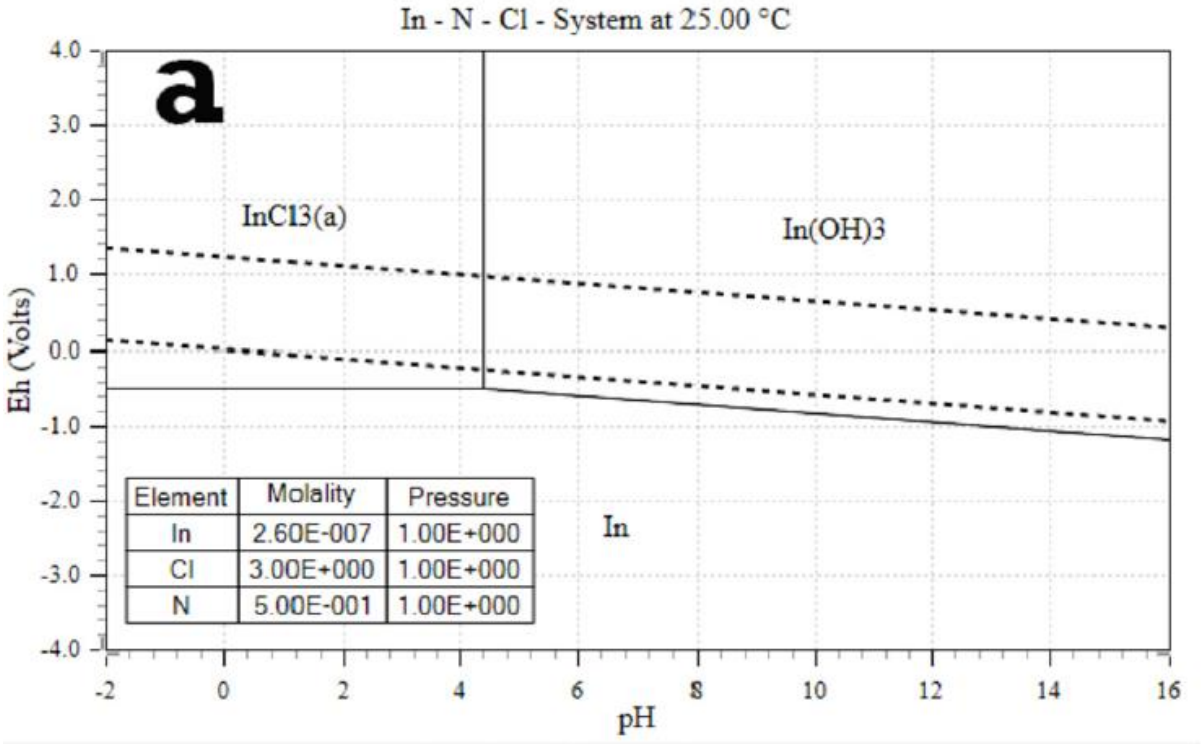

Figure 6: Eh-pH diagram (Assefi et al., 2018)

A 20 mg/L indium solution was obtained by dissolving indium chloride powder in distilled water. The solution was used to study the pH effect on the resin uptake. To set the optimum pH of the working solution, a dose of 10 mg of the IDA-modified chitosan was measured, put in a 10 mL tube and filled to the last mark i.e., 10 mL with the previously prepared solution at pH range of 0-4. The mixing took place in a shaker for 24 h at the ambient temperature. After the equilibrium was achieved, the samples were filtered and analysed with ICP.

6.2 Fourier transform infrared spectroscopy

Using Perkin Elmer Frontier spectrometer equipped with a universal ATR module (Diamond crystal), the FTIR spectra of both pure and modified chitosan powder and pure IDA were characterized to verify the presence of IDA in the modified chitosan powder. Each sample were measured thrice in absorbance mode at the wavenumber range of 4000−400 cm^{-1} with

the acquisition of 4 scans and in the data interval of 1 cm^{-1}. Ultimately, all the recorded spectra were processed with ATR and baseline correction.

6.3 Adsorption process

After determining the optimal pH value, the isotherm study was carried out to investigate the adsorbent capacities as well as the model of adsorption. Different concentrations of indium chloride were prepared at pH value of 3.5 and were added to a previously balanced 20 mg of IDA-chitosan in 10 mL tube and mixed for 24 hrs. Afterwards, the samples were filtered using syringe filters and analysed with ICP to determine the indium uptake. The obtained data were then processed and analysed and used to calculate the equilibrium adsorption capacities using Eq. 1.

For the kinetics study, a concentration range of 90-110 mg/L was selected, 20 mg of the adsorbent was placed in 10 mL tube and shook for certain periods 5-4320 min. The samples were filtered and analysed with ICP and the data were then processed, analysed and used to obtain the kinetics behaviour.

6.4 Desorption and regeneration

The desorption test was carried out after the adsorption of 100 mg/L of indium on 100 mg of IDA-Chitosan utilising 1 M of HCl as an eluent. The spent resin was rinsed several times with deionized water, filtered with centrifuge, and mixed with 1M of HCl for several cycles to test the desorption. The reusability test took place after the resin was desorbed and conditioned with deionized water, to test the adsorption again with 100 ppm solution. The contact time for this test was 12 hours in 350 rpm.

7 RESULTS AND DISCUSSION

This chapter comprises the functionalization assessment of IDA-chitosan as well as the adsorption process of indium chloride solution onto it, including the pH dependency, the isotherms study, the kinetics study, and the desorption and regeneration study respectively.

7.1 FT-IR IDA-chitosan Characterization

The spectra of the pure chitosan, the pure IDA, and IDA modified chitosan are illustrated in Figure 7 throughout a wavelength range of 4000−400 cm−1. It can be remarked that most of the IDA peaks overlap with the pure chitosan peaks due to the functional groups similarities. Nonetheless, a clear increasing trend in intensity of chitosan peaks can be noticed as IDA incorporated to the structure of chitosan, i.e. broad band at 3500−3200 cm^{-1} associated with the stretching vibration of the hydroxyl group O−H. The most clearly the effect of IDA on the FTIR spectrum of IDA modified chitosan can be seen at two wave numbers at 1578 and 1705 cm^{-1} which are the identical peaks assigned to (C=O) vibrations for IDA. As can be seen from Figure 7, these peaks reveal the existence of IDA in the formula of modified chitosan as υ (vibration) of (C=O) functional group is only present in the structure of IDA.

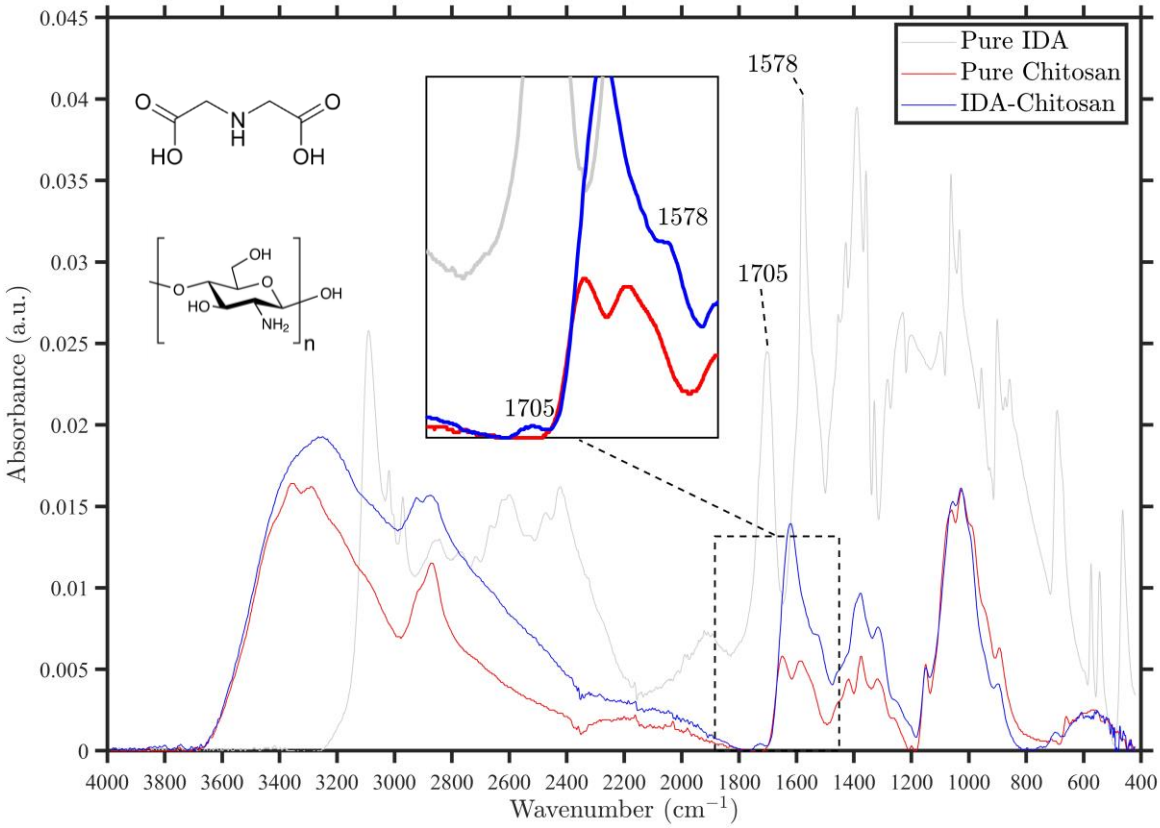

Figure 7: FTIR spectra of pure chitosan, pure IDA, and IDA modified chitosan throughout the range of 4000–400 cm−1. The peaks corresponding to the presence of IDA in modified chitosan can be clearly distinguished at 1705 and 1578 cm^{-1}.

7.2 pH effect on the adsorption

The pH is one of the most determinant factors on the adsorption process of indium ions from liquid solutions as it affects the surface group protonation as well as the degree of metal ionization (Hokkanen et al., 2013). Hence, the optimum pH value of the adsorption process must be determined first and foremost (Zhao et al., 2015). Moreover, due to the speciation of the indium chloride solution at a pH value above 4, the pH above this value was not considered at the present study (Assefi et al., 2018). In this study, 30 mg/L indium solution was added to 10 mg of the IDA-chitosan sorbent and the pH range to be considered was between 0.5 and 3.5, the samples were mixed for 24 h to make sure the equilibrium has been attained. After the adsorption, the samples were filtered and analysed with the ICP.

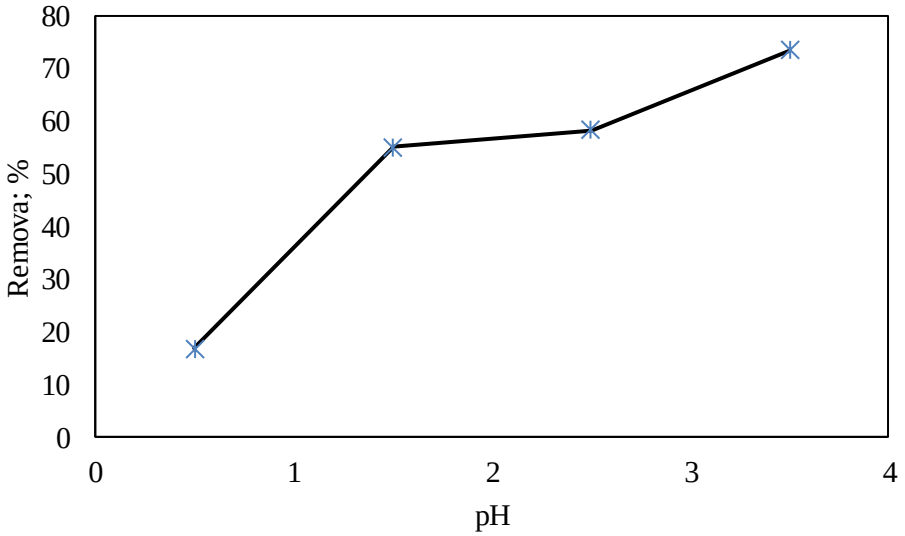

Figure 8: pH effect on the metal removal

It can be remarked from Figure 8 that the minimal adsorption efficiency was recorded in the lowest pH value. This is mainly due to elevated concentration of the hydronium ions, which intensifies the indium-protons competition for the adsorption sites, and ultimately hinders the metal uptake by the sorbent at lower pH values. On the other hand, the protonation of the solution decreases leading to increment in the adsorption sites and ultimate enhancement of the metal uptake. Consequently, the optimum pH value of this study was chosen to be the highest value i.e. 3.5. This result is analogous to those obtained by the literature as depicted by the following Table 5

Table5: comparative optimum pH value on various resins

pH value	Adsorbent	reference
3.5	IDA-chitosan	Present study
3.5	MEDCS/MDTCS	(Zhao et al., 2015)
3.5	Chelating cellulose	(Akama et al., 2016)
3.5	Phosphorylated sawdust	(Jeon et al., 2015)
4.0	Chitosan-Coated Bentonite Beads	(Calagui et al., 2014b)

As an outcome of the pH study, the pH value of 3.5 was selected as the optimum value and used in further experiments.

7.3 Isotherm study

Adsorption isotherms are used to depict the adsorption capacity of the adsorbent in correlation to the metal concentration in the solutions at the equilibrium conditions (Zhao et al., 2013b). Further, their give an insight to the adsorbate-adsorbent relationship when the in equilibrium conditions (Calagui et al., 2014b). To calculate the adsorption isotherm parameters, the experimental readings were fitted by using the most common three types of Error functions i.e. (EAB),(HYBRID), and (ERRSQ), and the latter one was adopted to calculate the isotherm parameters for its simplicity and common utilization in error analysis. Figure 9 depicts the adsorption experimental data and the isotherms models fitting of it.

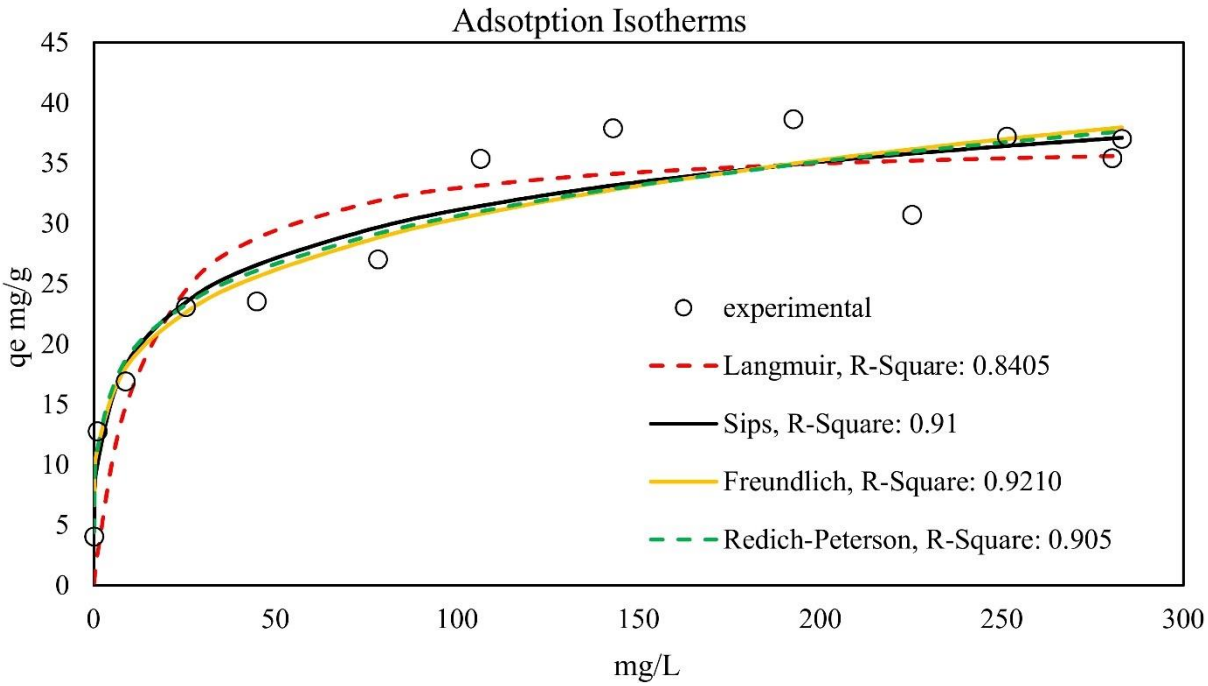

Figure 9: Experimental adsorption results fitted to Langmuir, Freundlich, Redlich-Peterson and Sips isotherm models

As illustrated by Figure 9 above, the highest R^2 value was obtained by Freundlich isotherm. In this case, the assumption of the adsorption will be that the adsorption takes place in a heterogeneous manner of the adsorbent surface with no saturation of the adsorption sites. However, the isotherm curve is still more or less trending and no clear equilibrium point can be deduced. This will lead to further consideration of Sips isotherm, the second highest R^2 value. Sips isotherm is applicable in case of the failure of Langmuir and Freundlich in the description of an adsorption process(Do, 1998). The Sips isotherm assumes the surface heterogeneity of the adsorption sites as well as the infinity of them (Reddy and Lee, 2013).

Nevertheless, the model profile has not reached a plateau and hence, no equilibrium point was achieved as in the case of Freundlich isotherm. Moreover, the calculated adsorption capacity was very high compared to the capacity obtained by the experimental data. Redlich-Peterson, presumes a mixed adsorption mechanism that does not adhere to Langmuir's mon layer adsorption same as the previous two isotherms (Nimibofa et al., 2017). Redlich-Peterson isotherm profile suffers undefined equilibrium like the previous Freundlich and Sips isotherms, what implies a further consideration of Langmuir isotherm.

Ultimately, as the indium adsorption onto IDA-modified chitosan was best fitted by the classical and commonly used Langmuir isotherm model. It can also be noticed from the Figure 9 above, that increment on the adsorption capacity is dependent on the increment of the equilibrium concentration in the beginning of the adsorption which is tend to be fixed at the high concentration due to the formation of a layer of indium on the IDA-chitosan surface.

Isotherms parameters were calculated by using ERRSQ function and the R^2 values were obtained by MATLAB curve-fitting tool, the obtained value and isotherms parameters are shown in Table 6 below.

Table 6:Isotherms Parameters for IDA-Chitosan adsorption

Isotherm	constants		R^2
Langmuir	$K_{L\ (L/mg)}$	0.07	0.8405
	$q_{m\ (mg/g)}$	37.267	
Freundlich	$K_{F\ (mg/g)}$	11.323	0.921
	B_F	0.214	
Sips	$K_{S\ (L/mg)}$	0.006	0.91
	β_s	0.342	
	q_m	67.659	
Redlich-Peterson	K_R	128.89	0.905
	β	0.803	
	A_R	10.385	

Since Langmuir isotherm gave the best fit with the experimental data, it was chosen to predict the adsorption behaviour of indium onto IDA-modified chitosan. Therefore a homogeneous monolayer distribution of the indium ions throughout the IDA-Chitosan surface can be assumed. This conclusion is comparable to the several chitosan based and indium adsorption studies as illustrated by Table 7 below.

Table 7: Comparative Langmuir constants for various studies

Study	Adsorbent	K_L [unit]	q_m [unit]
(Calagui et al., 2014b)	CCB	0.06 L/mg	17.89
(Jeon et al., 2015)	Phosphorylated sawdust	8.724 L/mg	1.121 mg/g
(Kwak et al., 2012a)	Microbeads	2.75-4.69 L/g	0.5 mmol/g
(Inoue et al., 2008)	SIRs	-	0.45 mmol/g
This study	IDA-Chitosan	0.07	37.9

7.4 Kinetics study

The contact time effect on the indium uptake onto IDA-Chitosan is illustrated by Figure 10 bellow. At the beginning of the adsorption, the indium uptake took place in a brisk manner owing to the abundance of free adsorption sites, gradually, the adsorption rate decreased as the indium metal occupied the adsorption sites and reached an equilibrium after 33 hrs.

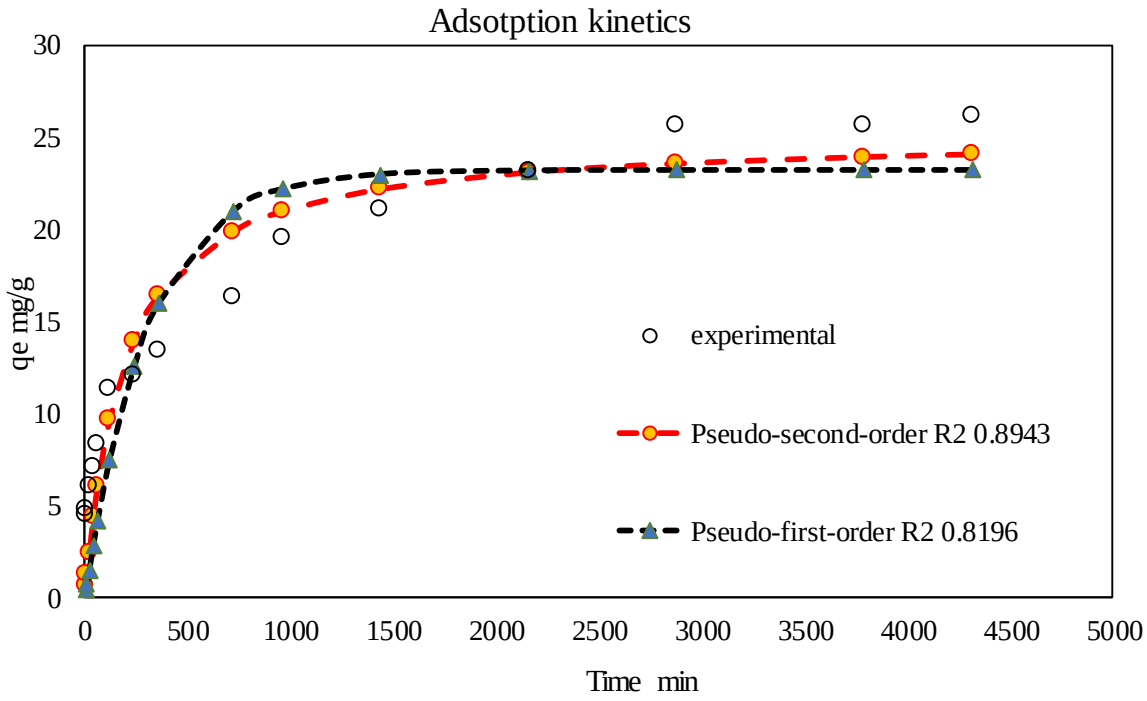

Figure 10: The effect of the contact time of indium ions adsorption by IDA-Chitosan

The Adsorption kinetics was assessed via pseudo-first and pseudo-second order kinetics models. The models parameters were calculated by using the (ERRSQ) error function and demonstrated in Table 8 below. The pseudo-second order model gave a better representation of the adsorption data with R^2 value closer to the unity and a higher correlation to the experimental maximum adsorption capacity. This implies a chemisorption of the indium ions on the IDA-Chitosan and is correlated to the findings of other authors for both chitosan-based sorbents and indium adsorption processes (Zhao et al., 2013b),(Repo et al., 2010b), and (Calagui et al., 2014b).

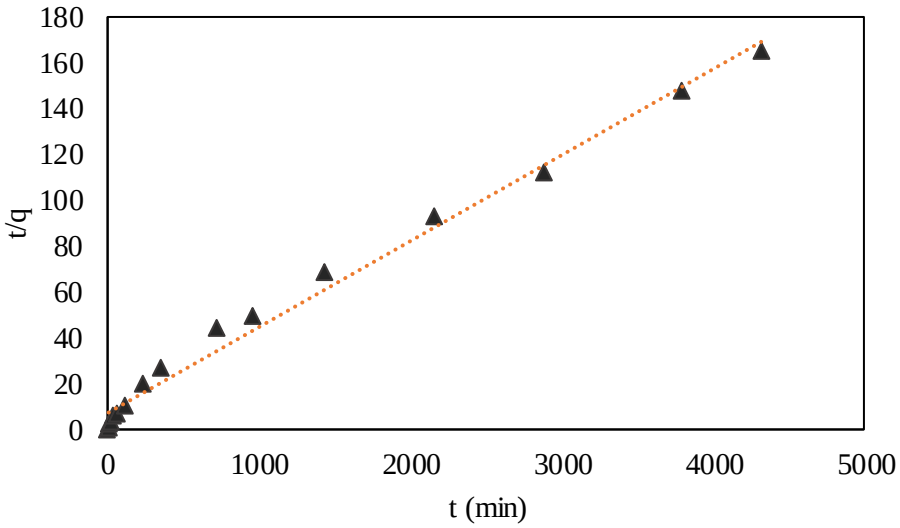

Figure 11: kinetic modelling of indium ions by IDA-Chitosan using pseudo-second order model

For further comprehension into the mechanism of the adsorption process, the intra-particle diffusion kinetic model was investigated and the figures below were obtained alongside the model parameters in Table 8.

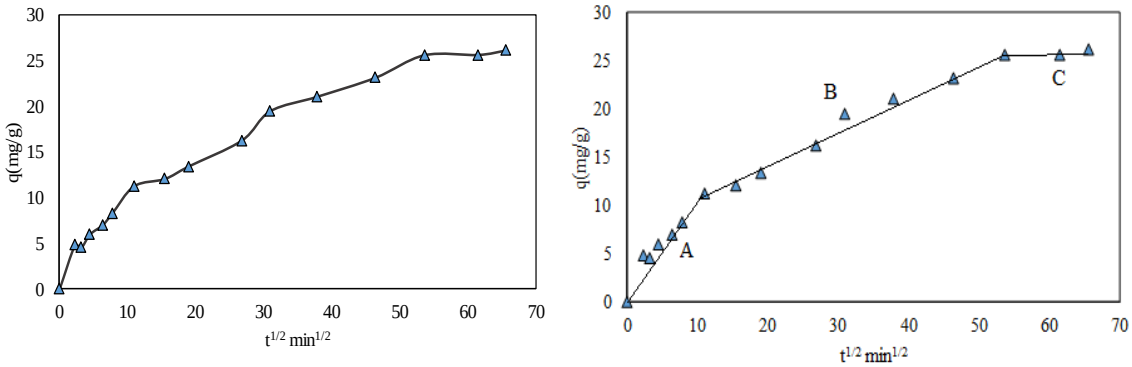

Figure 12 kinetic modelling of indium ions by IDA-Chitosan using intra-particle diffusion model

To ascertain the rate limiting step of the adsorption, intra-particle diffusion study was conducted by plotting q_t Vs $t^{1/2}$, to reveal a multi-linear profile trend as shown in Figure 12 above (on the right). Thus, the adsorption is assumed to take place in three phases as follows, the first steep line (zone A) represents the initial phase, which demonstrates the surface diffusion, accompanied by the gradual line (zone B) which represents the gradual capture of indium ions, and the mechanism in this phase can be related to the intra-particle diffusion. The last phase (Zone C) represent the achievement of the equilibrium. It can be concluded that the adsorption mechanism is controlled by the aforementioned three mechanisms. This conclusion is analogous to the results obtained by Olu-Owolabi et al. (2014).

Table 8:kinetics constants for IDA-Chitosan adsorption

kinetics model	constants		R^2
Pseudo-first order	K_1	0.003243	0.8196
	$q_{e\ (mg/g)}$	23..2126	
Pseudo-second order	K_2	0.000207	0.8943
	$q_{e\ (mg/g)}$	25.1317	
Intra-particle diffusion	$C_{(mg/g)}$	7.000	0.991
	K_{id}	0.0377	

To be concluded, the lower obtained K_2 indicates that the time required to achieve the equilibrium is relatively high which is also easily seen from the experimental data. As for the intra-particle diffusion model, a sufficient analogy can be conducted to the results obtained by Ho (2004). The intra-particle diffusion rate and curve manifestation propose both instantaneous external surface capture of the indium and a slower intra-particle indium diffusion, and the latter one is assumed to be the rate controlling step.

7.5 Desorption and reusability

To complete the recovery cycle, the adsorbed meal ions were eluded using HCl and HNO_3 at 1M, as an eluent. The metal ions were desorbed in 7 cycles for HCl as presented in Table 9 below. As for the reusability, adsorbent was rinsed with deionized water for 10 mins and separated with the centrifuge and used three times to test the reusability. The results revealed almost one third as a cut-off in the metal uptake assumed to be caused by the eluent high concentration. This suggests that further investigation of the procurement of other eluents is needed.

Table 9: Regeneration of IDA-chitosan by 1 M of HCl

Cycle number	q_e before the regeneration (mg/g)	q_e after the regeneration (mg/g)	Regeneration efficiency (%)
1	22.56485	14.83611	65.78
2	22.56485	14.5077	64.27
3	22.56485	14.31506	63.43
4	22.56485	12.42658	55.05

Table 9 above shows severe deterioration in the regeneration assumed to be caused by the eluent high concentration that led to the decomposition of the IDA functionality.

8 CONCLUSIONS

The aim of this study was to investigate the modification of chitosan with Iminodiacetic acid chelating agent, and to further test its affinity towards indium ions, expanding the adsorption process to have a clear insight on the affecting factors of the process starting from the determination of the optimum pH, the isotherm, the kinetics, the elusion and the regeneration of the spent adsorbent. Firstly, the adsorbent functionalization was approved by the FTIR spectra by feeding the pure chitosan, pure IDA and the IDA-modified chitosan. The adsorption study revealed that the optimum pH value for the adsorption is 3.5 due to the indium chloride speciation at pH value of 4 as well as the indium ions uptake was at the highest value 37.9 mg/g at this pH. Further, indium adsorption was studied over several isotherm models, and was found to follow the Langmuir model. Subsequently, the adsorption capacity was concluded to be 37.9 mg/g, while the adsorption kinetics study the deduced pseudo-second order model with 3000 min as equilibrium time. However, it was shown that diffusion was also playing a significant role as a rate limiting step. The elusion of the adsorbed indium ions procured using 1 M of HCl and the metal breakthrough point was remarked on the 7^{th} cycle. Ultimately, the spend IDA-Chitosan was conditioned and reused for 5 times with a considerable deterioration in the efficiency after the third regeneration cycle.

As a result of this study, successful modification of Chitosan with Iminodiacetic acid, further, IDA-modified chitosan was shown. The produced material was found to be suitable to be used to capture indium ions from indium chloride solution. Thus, it can be concluded that IDA-Chitosan showed a potential prospects of utilization as an adsorbent in to reclaim the metal ions Further investigations about the indium coordination with IDA-Chitosan, as well as the temperature effects of adsorption behaviour are still needed. In addition, the stability of the new adsorbent should be investigated in order to find out optimal conditions for its regeneration, which is highly important from the practical point of view.

9 REFERENCES

Adsorption of Vapors on Minerals and Other Solids. *Partition and Adsorption of Organic Contaminants in Environmental Systems.*

2011. Critical Metals in Strategic Energy Technologies - Assessing Rare Metals as Supply-Chain Bottlenecks in Low-Carbon Energy Technologies. Publications Office of the European Union.

2015. Recent Modifications of Chitosan for Adsorption Applications: A Critical and Systematic Review. *marine drugs***,** 312-337.

2019. IntechOpen. Available: https://cdn.intechopen.com/pdfs/61572.pdf [Accessed 10 27].

A.M. ALFANTAZI, R. R. M. B. 2003. *Processing of indium: a review*.

ADHIKARI, B. B., GURUNG, M., KAWAKITA, H. & OHTO, K. 2012. Solid phase extraction, preconcentration and separation of indium with methylene crosslinked calix[4]- and calix[6]arene carboxylic acid resins. *Chemical Engineering Science,* 78**,** 144-154.

AKAMA, Y., SUZUKI, S. & MONOBE, Y. 2016. Study on the adsorption and selective separation of indium from zinc with chelating cellulose. *Cellulose Chemistry and Technology,* 50**,** 147-152.

ALGUACIL, F. J., LOPEZ, F. A., RODRIGUEZ, O., MARTINEZ-RAMIREZ, S. & GARCIA-DIAZ, I. 2016. Sorption of indium (III) onto carbon nanotubes. *Ecotoxicology and Environmental Safety,* 130**,** 81-86.

ALLEN, S. J., MCKAY, G. & PORTER, J. F. 2004. Adsorption isotherm models for basic dye adsorption by peat in single and binary component systems. *Journal of Colloid and Interface Science,* 280**,** 322-333.

ASSEFI, M., MAROUFI, S., NEKOUEI, R. K. & SAHAJWALLA, V. 2018. Selective recovery of indium from scrap LCD panels using macroporous resins. *Journal of Cleaner Production,* 180**,** 814-822.

BARNABAS, M. J., PARAMBADATH, S., MATHEW, A., PARK, S. S., VINU, A. & HA, C.-S. 2016. Highly efficient and selective adsorption of In3+ on pristine Zn/Al layered double hydroxide (Zn/Al-LDH) from aqueous solutions. *Journal of Solid State Chemistry,* 233**,** 133-142.

BUSEV, A. I. 1962. *The Analytical Chemistry of Indium*, PERGAMON Press.

C. B. FORTES, M., H. MARTINS, A. & S. BENEDETTO, J. 2007. Selective separation of indium by iminodiacetic acid chelating resin. *Brazilian Journal of Chemical Engineering - BRAZ J CHEM ENG,* 24.

CALAGUI, M. J., SENORO, D., KAN, C.-C., SALVACION, J., FUTALAN, C. & WAN, M.-W. 2014a. Adsorption of Indium (III) ions from aqueous solution using chitosan-coated bentonite beads. *Journal of hazardous materials,* 277.

CALAGUI, M. J. C., SENORO, D. B., KAN, C.-C., SALVACION, J. W. L., FUTALAN, C. M. & WAN, M.-W. 2014b. Adsorption of indium(III) ions from aqueous solution using chitosan-coated bentonite beads. *Journal of Hazardous Materials,* 277**,** 120-126.

CHANG, X., SU, Z., LUO, X. & ZHAN, G. 1993. Synthesis of poly(acrylamidrazone-hydrazide) chelating fiber and application of enrichment—separation for traces of indium, tin, chromium, vanadium and titanium from solution samples. *Talanta,* 40**,** 527-532.

CHOONG JEON, J.-H. C. A., JAE-YOUNG CHOI 2015. Adsorption and recovery characteristics of phosphorylated sawdust bead for indium(III) in industrial wastewater. *Journal of Industrial and Engineering Chemistry*.

DO, D. D. Adsorption analysis : equilibria and kinetics. Imperial College Press.

FELIX, N. 1990. *Indium and Indium Compounds*.

FERELLA, F., BELARDI, G., MARSILII, A., DE MICHELIS, I. & VEGLIÒ, F. 2017. Separation and recovery of glass, plastic and indium from spent LCD panels. *Waste Management,* 60**,** 569-581.

FERSHMAN, A. Y. 1953. *Geochemical and mineralogical methods of prospecting for mineral resources*.

FONTANA, D., FORTE, F., DE CAROLIS, R. & GROSSO, M. 2015. Materials recovery from waste liquid crystal displays: A focus on indium. *Waste Management,* 45**,** 325-333.

FOO, K. Y. & HAMEED, B. 2010a. Insights into Modeling of Adsorption Isotherm Systems. *Chemical Engineering Journal,* 156**,** 2-10.

FOO, K. Y. & HAMEED, B. H. 2010b. Insights into the modeling of adsorption isotherm systems. *Chemical Engineering Journal,* 156**,** 2-10.

GILES, C. H., SMITH, D. & HUITSON, A. 1974. A general treatment and classification of the solute adsorption isotherm. I. Theoretical. *Journal of Colloid and Interface Science,* 47**,** 755-765.

GUAN, J., WANG, S., REN, H., GUO, Y., YUAN, H., YAN, X., GUO, J., GU, W., SU, R., LIANG, B., GAO, G., ZHOU, Y., XU, J. & GUO, Z. 2015. Indium recovery from waste liquid crystal displays by polyvinyl chloride waste. *RSC Advances,* 5**,** 102836-102843.

HASEGAWA, H., RAHMAN, I. M. M., UMEHARA, Y., SAWAI, H., MAKI, T., FURUSHO, Y. & MIZUTANI, S. 2013. Selective recovery of indium from the etching waste solution of the flat-panel display fabrication process. *Microchemical Journal,* 110**,** 133-139.

HAYES, S. M. & MCCULLOUGH, E. A. 2018. Critical minerals: A review of elemental trends in comprehensive criticality studies. *Resources Policy,* 59**,** 192-199.

HO, Y.-S. 2004. Comment on “Removal of copper from aqueous solution by aminated and protonated mesoporous aluminas: kinetics and equilibrium,” by S. Rengaraj, Y. Kim, C.K. Joo, and J. Yi. *Journal of Colloid and Interface Science,* 276**,** 255-258.

HO, Y.-S. 2006. Second-order kinetic model for the sorption of cadmium onto tree fern: A comparison of linear and non-linear methods. *Water Research,* 40**,** 119-125.

HOKKANEN, S., REPO, E. & SILLANPÄÄ, M. 2013. Removal of heavy metals from aqueous solutions by succinic anhydride modified mercerized nanocellulose. *Chem. Eng. J.,* 223**,** 40.

INOUE, K., NISHIURA, M., KAWAKITA, H., OHTO, K. & HARADA, H. 2008. Recovery of Indium from Spent Panel of Liquid Crystal Display Panels. *Kagaku Kogaku Ronbunshu,* 34**,** 282-286.

JEON, C., CHA, J.-H. & CHOI, J.-Y. 2015. Adsorption and recovery characteristics of phosphorylated sawdust bead for indium(III) in industrial wastewater. *Journal of Industrial and Engineering Chemistry,* 27**,** 201-206.

KANG, H. N., LEE, J.-Y. & KIM, J.-Y. 2011. Recovery of indium from etching waste by solvent extraction and electrolytic refining. *Hydrometallurgy,* 110**,** 120-127.

KWAK, N.-S., BAEK, Y. & HWANG, T. S. 2012a. The synthesis of poly(vinylphosphonic acid-co-methacrylic acid) microbeads by suspension polymerization and the characterization of their indium adsorption properties. *Journal of Hazardous Materials,* 203-204**,** 213-220.

KWAK, N.-S., PARK, H.-M. & HWANG, T. S. 2012b. Preparation of ion-exchangeable nanobeads using suspension polymerization and their sorption properties for indium in aqueous solution. *Chemical Engineering Journal,* 191**,** 579-587.

L. TIMOFEEV, K., I. MALTSEV, G., V. USOLTSEV, A. & S. NABOICHENKO, S. 2017. Sorption technology of indium extraction from zinc production solutions. *Izvestiya Vuzov Tsvetnaya Metallurgiya (Proceedings of Higher Schools Nonferrous Metallurgy***,** 43-50.

LEE, S.-K. & LEE, U. H. 2016. Adsorption and Desorption Property of Iminodiacetate Resin (Lewatit® TP207) for Indium Recovery. *Journal of Industrial and Engineering Chemistry,* 40.

LI, H., LIU, J., GAO, X., LIU, C., GUO, L., ZHANG, S., LIU, X. & LIU, C. 2012. Adsorption behavior of indium(III) on modified solvent impregnated resins (MSIRs) containing sec-octylphenoxy acetic acid. *Hydrometallurgy,* 121-124**,** 60-67.

LI, J., GAO, S., DUAN, H. & LIU, L. 2009. Recovery of valuable materials from waste liquid crystal display panel. *Waste Management,* 29**,** 2033-2039.

LI, M., FENG, C., LI, M., ZENG, Q. & GAN, Q. 2015. Synthesis and application of a surface-grafted In (III) ion-imprinted polymer for selective separation and pre-concentration of indium (III) ion from aqueous solution. *Hydrometallurgy,* 154**,** 63-71.

LI, R.-D., YUAN, T.-C., FAN, W.-B., QIU, Z.-L., SU, W.-J. & ZHONG, N.-Q. 2014. Recovery of indium by acid leaching waste ITO target based on neural network. *Transactions of Nonferrous Metals Society of China,* 24**,** 257-262.

LI, S.-Q., TANG, M.-T., HE, J., YANG, S.-H., TANG, C.-B. & CHEN, Y.-M. 2006. Extraction of indium from indium-zinc concentrates. *Transactions of Nonferrous Metals Society of China,* 16**,** 1448-1454.

LI, X.-H., ZHANG, Y.-J., QIN, Q.-L., YANG, J. & WEI, Y.-S. 2010. Indium recovery from zinc oxide flue dust by oxidative pressure leaching. *Transactions of Nonferrous Metals Society of China,* 20**,** s141-s145.

LI, Y., LIU, Z., LI, Q., LIU, Z. & ZENG, L. 2011. Recovery of indium from used indium–tin oxide (ITO) targets. *Hydrometallurgy,* 105**,** 207-212.

LIDE, D. R. *CRC Handbook of Chemistry and Physics*, CRC Press LLC 2005.

LIMOUSIN, G., GAUDET, J. P., CHARLET, L., SZENKNECT, S., BARTHÈS, V. & KRIMISSA, M. 2007. Sorption isotherms: A review on physical bases, modeling and measurement. *Applied Geochemistry,* 22**,** 249-275.

LIU, H.-M., WU, C.-C., LIN, Y.-H. & CHIANG, C.-K. 2009. Recovery of indium from etching wastewater using supercritical carbon dioxide extraction. *Journal of Hazardous Materials,* 172**,** 744-748.

LOKANC, M., EGGERT, R. & REDLINGER, M. 2015. The Availability of Indium: The Present, Medium Term, and Long Term. United States.

LÓPEZ-YÁÑEZ, A., ALONSO, A., VENGOECHEA-PIMIENTA, A. & RAMÍREZ-MUÑOZ, J. 2019. Indium and tin recovery from waste LCD panels using citrate as a complexing agent. *Waste Management,* 96**,** 181-189.

MAEDA, H. & EGAWA, H. 1991. Removal and recovery of gallium and indium lons in acidic solution with chelating resin containing aminomethylphosphonic acid groups. *Journal of Applied Polymer Science,* 42**,** 737-741.

MAITY, J. & RAY, S. K. 2018. Chitosan based nano composite adsorbent—Synthesis, characterization and application for adsorption of binary mixtures of Pb(II) and Cd(II) from water. *Carbohydrate Polymers,* 182**,** 159-171.

MARINHO, R. S., SILVA, C. N. D., AFONSO, J. C. & CUNHA, J. W. S. D. D. 2011. Recovery of platinum, tin and indium from spent catalysts in chloride medium using strong basic anion exchange resins. *Journal of Hazardous Materials,* 192**,** 1155-1160.

MOHAMMAD ASSEFI, S. M., RASOUL KHAYYAM NEKOUEI, VEENA SAHAJWALLA 2018. Selective recovery of indium from scrap LCD panels using. *Journal of Cleaner Production,* 180**,** 814-822.

MOSS, R. L., KARA, H., WILLIS, P. & KOOROSHY, J. 2012. Critical Metals in Strategic Energy Technologies Assessing Rare Metals as Supply-Chain Bottlenecks in Low-Carbon Energy Technologies.: JRD Scientific and Technical Reports.

NG, J. C. Y., CHEUNG, A. & MCKAY, G. 2002. Equilibrium Studies of the Sorption of Cu(II) Ions onto Chitosan. *Journal of colloid and interface science,* 255**,** 64-74.

NIMIBOFA, A., EBELEGI, A. & DONBEBE, W. 2017. Modelling and Interpretation of Adsorption Isotherms. *Hindawi Journal of Chemistry,* Volume 2017**,** 11 pages.

NREL 2017. *The Availability of Indium:The present, Medium term and Long term*

OLU-OWOLABI, B. I., DIAGBOYA, P. N. & ADEBOWALE, K. O. 2014. Evaluation of pyrene sorption–desorption on tropical soils. *Journal of Environmental Management,* 137**,** 1-9.

PAIVA, A. P. 2001. RECOVERY OF INDIUM FROM AQUEOUS SOLUTIONS BY SOLVENT EXTRACTION. *Separation Science and Technology,* 36**,** 1395-1419.

PLAZINSKI, W., RUDZINSKI, W. & PLAZINSKA, A. 2009. Theoretical models of sorption kinetics including a surface reaction mechanism: A review. *Advances in Colloid and Interface Science,* 152**,** 2-13.

PÉREZ-MARÍN, A. B., ZAPATA, V. M., ORTUÑO, J. F., AGUILAR, M., SÁEZ, J. & LLORÉNS, M. 2007. Removal of cadmium from aqueous solutions by adsorption onto orange waste. *Journal of Hazardous Materials,* 139**,** 122-131.

RAZAK, M. R., YUSOF, N. A., HARON, M. J., IBRAHIM, N., MOHAMMAD, F., KAMARUZAMAN, S. & AL-LOHEDAN, H. A. 2018. Iminodiacetic acid modified kenaf fiber for waste water treatment. *International Journal of Biological Macromolecules,* 112**,** 754-760.

REDDY, D. H. & LEE, S.-M. 2013. Synthesis and Characterization of a Chitosan Ligand for the Removal of Copper from Aqueous Media. *Journal of Applied Polymer Science,* 130.

REPO, E., WARCHOL, J. K., KURNIAWAN, T. A. & SILLANPÄÄ, M. E. T. 2010a. Adsorption of Co(II) and Ni(II) by EDTA- and/or DTPA-modified chitosan: Kinetic and equilibrium modeling. *Chem. Eng. J.,* 161**,** 73.

REPO, E., WARCHOL, J. K., KURNIAWAN, T. A. & SILLANPÄÄ, M. E. T. 2010b. Adsorption of Co(II) and Ni(II) by EDTA- and/or DTPA-modified chitosan: Kinetic and equilibrium modeling. *Chemical Engineering Journal,* 161**,** 73-82.

REPO, E., WARCHOŁ, J. K., BHATNAGAR, A. & SILLANPÄÄ, M. 2011. Heavy metals adsorption by novel EDTA-modified chitosan–silica hybrid materials. *J. Colloid Interface Sci.,* 358**,** 261.

RINAUDO, M. 2006. Chitin and chitosan: Properties and applications. *Progress in Polymer Science,* 31**,** 603-632.

SAMI VIROLAINEN, D. I. 2011. Recovery of indium from indium tin oxide by solvent extraction. *Hydrometallurgy*.

SAWAI, H., RAHMAN, I. M. M., TSUKAGOSHI, Y., WAKABAYASHI, T., MAKI, T., MIZUTANI, S. & HASEGAWA, H. 2015. Selective recovery of indium from lead-smelting dust. *Chemical Engineering Journal,* 277**,** 219-228.

SEN GUPTA, S. & BHATTACHARYYA, K. G. 2011. Kinetics of adsorption of metal ions on inorganic materials: A review. *Advances in Colloid and Interface Science,* 162**,** 39-58.

SONG, Q., ZHANG, L. & XU, Z. 2020. Indium recovery from In-Sn-Cu-Al mixed system of waste liquid crystal display panels via acid leaching and two-step electrodeposition. *Journal of Hazardous Materials,* 381**,** 120973.

SWAIN, B., MISHRA, C., HONG, H. S. & CHO, S.-S. 2016. Beneficiation and recovery of indium from liquid-crystal-display glass by hydrometallurgy. *Waste Management,* 57**,** 207-214.

USGS 2016. *USGS (U.S. Geological Survey), 2016. Mineral Commodity Summaries.*

WROŃSKI, G., DEBCZAK, A. & HUBICKI, Z. 2009. Application of the FT-IR/PAS method in comparison of Ga(III) and In(III) sorption on lewatit OC-1026 and amberlite XAD-7 impregnated D2EHPA. *Acta Physica Polonica A,* 116**,** 435.

XIONG, C. & YAO, C. 2008. Sorption behavior of iminodiacetic acid resin for indium. *Rare Metals,* 27**,** 153-157.

YANG, J., EKBERG, C. & RETEGAN, T. 2014. Optimization of Indium Recovery and Separation from LCD Waste by Solvent Extraction with Bis(2-ethylhexyl) Phosphate (D2EHPA). *International Journal of Chemical Engineering,* 2014**,** 9.

YANG, J., RETEGAN, T. & EKBERG, C. 2013. Indium recovery from discarded LCD panel glass by solvent extraction. *Hydrometallurgy,* 137**,** 68-77.

YUAN, Y., LIU, J., ZHOU, B., YAO, S., LI, H. & XU, W. 2010. Synthesis of coated solvent impregnated resin for the adsorption of indium (III). *Hydrometallurgy,* 101**,** 148-155.

ZHAO, F., REPO, E., SILLANPÄÄ, M., MENG, Y., YIN, D. & TANG, W. Z. 2015. Green Synthesis of Magnetic EDTA- and/or DTPA-Cross-Linked Chitosan Adsorbents for Highly Efficient Removal of Metals. *Industrial & Engineering Chemistry Research,* 54**,** 1271-1281.

ZHAO, F., REPO, E., YIN, D. & SILLANPÄÄ, M. E. T. 2013a. Adsorption of Cd(II) and Pb(II) by a novel EGTA-modified chitosan material: Kinetics and isotherms. *J. Colloid Interface Sci.,* 409**,** 174.

ZHAO, F., REPO, E., YIN, D. & SILLANPÄÄ, M. E. T. 2013b. Adsorption of Cd(II) and Pb(II) by a novel EGTA-modified chitosan material: Kinetics and isotherms. *Journal of Colloid and Interface Science,* 409**,** 174-182.

ZICHAO LIA, G. L. D., ABDULLAH BAJAHZARC,⁎, LOTFI SELLAOUID,⁎, HAFEDH BELMABROUKE, 2019. Adsorption of indium (III) from aqueous solution on raw, ultrasound- and supercritical-modified chitin: Experimental and theoretical analysis. *Chemical Engineering Journal* 373**,** 1247-1253.